Published in Sedimentary Geology
Volume 425, November 2021, 106005
Link to the publisher version: https://www.sciencedirect.com/science/article/pii/S0037073821001573

Skeletal assemblages and terrigenous input in the Eocene carbonate systems of the Nummulitic Limestone (NW Europe)

Giovanni Coletti [a,*], Luca Mariani [a], Eduardo Garzanti [a], Sirio Consani [b], Giulia Bosio [a], Giovanni Vezzoli [a], Xiumian Hu [c], Daniela Basso [a]

[a] Department of Earth and Environmental Sciences, University of Milano-Bicocca, Piazza della Scienza 4, 20126 Milano, Italy
[b] DISTAV, University of Genova, Corso Europa, 26, 16132 Genova, Italy
[c] State Key Laboratory of Mineral Deposits Research, School of Earth Sciences and Engineering, Nanjing University, Nanjing 210023, China

Terrigenous input is often considered detrimental for carbonate producing organisms, however, the common occurrence of mixed siliciclastic–bioclastic deposits indicates that the relationship between carbonate factories and terrigenous fluxes is a complex issue. To investigate this subject, we analyzed the skeletal assemblages of the Paleogene Alpine foreland basin in a wide area encompassing NW Italy and SE France. Four different sections, Mortola, Loreto, Braux and Lauzanier, deposited between the Bartonian and the Priabonian, were studied in detail and, based on microfacies analysis, six main biofacies were recognized: i) nummulitid biofacies and ii) acervulinid and coralline algal biofacies related to shallow water; iii) nummulitid and orthophragminid biofacies and iv) coralline-algal branches and large benthic foraminifera biofacies related to intermediate depth; v) orthophragminid biofacies and vi) orthophragminid and coralline algal biofacies related to deeper settings. Thin sections and X-ray diffraction analyses show that these biofacies can be related to two major carbonate factories. The former was dominated by free-living benthic foraminifera and was characterized by a relevant terrigenous fraction, indicating free-living benthic foraminifera as the most terrigenous-tolerant group of carbonate producers of the Nummulitic Limestone system. The latter was dominated by encrusting acervulinids and coralline algae and thrived far-off major terrigenous sources. Conversely, recent and Neogene coralline algae are known to be able to tolerate high sedimentation rates. The distribution of coralline-algal-rich skeletal assemblages in the Nummulitic Limestone thus hints that Eocene coralline algae might have been fundamentally different (probably less adaptable) than their more modern counterparts.

Keywords: Paleogene; Carbonate factories; Foreland basin; Foraminifera; Acervulinids; Calcareous algae

1. Introduction

It is a common opinion that clastic input is detrimental for marine carbonate producing organism. This is based on three major pieces of evidence. First, most carbonate producers either feed by catching food from the water column (either passively like bryozoans or actively like corals), and thus they can be damaged by sediment ingestion (e.g., James and Kendall, 1992), or are dependent on light (e.g., calcareous algae, symbiont-bearing corals), and therefore they dislike turbid water and even more being covered in sediment. Secondly, most of them are sessile or they have a limited mobility, and thus, if buried by sediment, neither escaping nor relocating is an option. Last but not least, many large present-day carbonate systems are located far away from major sources of terrigenous sediment (e.g., the Bahamas Bank Complex, Roberts, 1987; the Maldive Islands, Lüdmann et al., 2013). Although the detrimental effect of clastic sediment is undeniable, carbonate production can take place even in areas with significant sediment influx, as testified by the common occurrence of mixed siliciclastic–bioclastic deposits (e.g., Doyle and Roberts, 1988; Wilson and Lokier, 2002; Lokier et al., 2009). One explanation for this apparent exception is that clastic input may be seasonal or episodic and a period of high supply can be followed by low accumulation sufficiently prolonged for a carbonate factory to develop (e.g., Bernasconi et al., 1997; Tomassetti et al., 2013). Another reason is that some carbonate-producing organisms are able to deal with high sedimentation rate. Red calcareous algae can photosynthesize even in dim light (e.g., van den Hoeck et al., 1995) and withstand sediment-related turbidity (e.g., Lokier et al., 2009). Larger benthic foraminifera can excavate themselves following shallow burial (e.g., Lokier et al., 2009). Corals are capable of cleaning their surface and remove sediment particles from their oral disk (e.g., solitary fungiids, Heikoop et al., 1996; *Cladocora caespitosa*, Schiller, 1993). The grain size of clastic material is another important variable,

because the self-cleaning capabilities of corals are strictly limited by particle grain-size (e.g., Lasker, 1980). Moreover, particle size affects micro-environmental dynamics (e.g., substrate stability, development of microbial biofilms) and consequently also affects the distribution of carbonate producers such as bryozoans and foraminifers (e.g., Smith, 1995; Du Châtelet et al., 2009).

Because sediment supply has a significant impact on both the development of carbonate factories and their composition, favoring certain groups over others, the interplay between skeletal-assemblage composition and abundance of clastic material can provide important paleoenvironmental information. Furthermore, because human activities (e.g., dam building, land development, deforestation) exert a significant impact on the sediment load of rivers, and thus on the amount of clastic material delivered to the sea, a full understanding of the response of carbonate factories to terrigenous fluxes is essential to foresee the long-term dynamics of modern environments.

This study aims at investigating the effects of terrigenous fluxes on carbonate-producing biota focusing on the Paleogene Alpine foreland basin. Foreland basins are created by dynamic forces related to continental subduction and by lithospheric flexure caused by the load of the orogen (Dickinson, 1974; DeCelles and Giles, 1996; Sinclair and Naylor, 2012; Garzanti, 2019a). The southwestern part of the Alpine foreland basin hosts extensive carbonate and mixed siliciclastic-carbonate successions, mainly deposited during the Eocene epoch and generally displaying an overall (and similar) deepening-upward trend controlled by tectonic subsidence (Ravenne et al., 1987; Sinclair, 1997). These successions, developed in a relatively small area, display a wide variety of carbonate facies and a remarkably variable terrigenous fraction, representing an ideal setting to study the effects of clastic input on carbonate-producing biota and highlight differences and similarities between Paleogene systems and their modern counterparts.

2. Geological setting

The Alpine foreland basin formed mainly as a consequence of the convergence of the European continent with the Adria microplate that created the Alps and next the Apennines, and extends from Liguria and southeastern France to Switzerland and Austria. In the study area, located at the political border between Italy and France (Fig. 1A, B), the strata underlying the foreland-basin succession consist of calcilutites, sandstones and minor microconglomeratic sandstones deposited by turbidity currents and debris flows in the quasi-oceanic Alpine Tethys seaway during the Late Cretaceous (Ravenne et al., 1987; Giammarino et al., 2010; Mueller et al., 2018) (Fig. 1C). These units are separated by a major angular unconformity from the overlying Paleogene deposits (Fig. 1C).

2.1. The Paleogene succession

The Paleogene succession can be broadly divided into six main units testifying to the evolution of the basin: 1) the Infranummulitic, 2) the Nummulitic Limestone, 3) the *Globigerina* Marls, 4) the Sandstones, 5) the Mélanges, and 6) the Molasse (Fig. 1C).

1) The Infranummulitic (locally named Infranummulitic Formation, *Microcodium* Formation, or Poudingues d'Argens) is generally 10 to 50 m thick (Sturani, 1965; Sinclair et al., 1998; Varrone and Clari, 2003; Barale et al., 2016), but thicker deposits have been reported in the western stretches of the basin (Barrême area; Ford et al., 1999). It displays a remarkable variety of sedimentary deposits related to fluvio-deltaic and very shallow marine environments (e.g., Sturani, 1965; Ravenne et al., 1987; Gupta, 1997; Sinclair et al., 1998; Evans and Elliott, 1999; Varrone and Clari, 2003). In the studied area, from the bottom to the top, the most common ones are: i) *Microcodium*-bearing marly breccias usually separated from the underlying substrate by an erosive surface and characterized by poorly sorted angular fragments of Upper Cretaceous marlstone and reworked Upper Cretaceous planktonic foraminifera (Varrone and Clari, 2003); ii) *Microcodium*-bearing marly limestone, locally nodular, displaying reworked Upper Cretaceous planktonic foraminifera and rare terrigenous grains (Sturani, 1965; Sinclair et al., 1998; Varrone and Clari, 2003); iii) *Microcodium*-bearing conglomerates, consisting of clast-supported lenticular deposits, mainly characterized by pebbles related to the erosion of the underlying Upper Cretaceous substrate (chert pebbles and very rare nummulitic limestone pebbles also occur) (Sturani, 1965; Sinclair et al., 1998; Varrone and Clari, 2003; Sztrákos and Du Fornel, 2003). Sand lenses have also been reported. These conglomerates also include a small bioclastic fraction consisting of reworked *Inoceramus* and rare *Nummulites* (Sinclair et al., 1998; Varrone and Clari, 2003); iv) clast-supported conglomerates with *Microcodium*-bearing pebbles locally displaying remains of terrestrial vertebrates (including *Palaeotherium* that indicates an age not older than the middle Eocene; Sturani, 1965); v) fine-grained dark limestones (also called *Cerithium* marlstones), characterized by lenses of dark-chert, terrestrial, brackish and shallow-marine gastropods, remains of charophytes, terrestrial plants and shallow-water benthic foraminifera (Sturani, 1965; Sinclair et al., 1998; Varrone and Clari, 2003; Sztrákos and Du Fornel, 2003). Gastropod assemblages suggest a Bartonian age for these deposits (Sturani, 1965); vi) well-sorted, quartz-rich sands displaying rare large benthic foraminifera (mainly *Nummulites brongnarti*, *Nummulites puschi*, *Nummulites striatus* and *Orbitolites*; indicating a Bartonian age; Serra-Kiel et al., 1998; Varrone and Clari, 2003). Since *Microcodium* consists of microscopic aggregates of elongated calcite crystals related to the decomposing activity of either roots, fungi or bacteria within the soil (Klappa, 1978; Košir, 2004; Kabanov et al., 2008), i, ii iii and iv should have formed in a continental environment (most likely a river valley) (Sturani, 1965; Gupta, 1997; Sinclair et al., 1998; Varrone and Clari, 2003; Sztrákos and Du Fornel, 2003); v should represent the transition toward a brackish or shallow marine environment, and vi should indicate fully marine conditions (Sturani, 1965; Sinclair et al., 1998; Varrone and Clari, 2003). Overall the facies succession of the Infranummulitic unit represents the initial phase of a marine transgression.
2) The Nummulitic Limestone, which represents the focus of this study, testifies to a widespread marine transgression. It is characterized by a variable thickness ranging between 10 and 100 m, generally greater in the external eastern part of the basin and decreasing westward (Sinclair et al., 1998; Evans and Elliott, 1999; Varrone and Clari, 2003; Sztrákos and Du Fornel, 2003), but it goes up to 150 m in western Liguria (Loreto area; Varrone and D'Atri, 2007). The Nummulitic Limestone lies unconformably either onto the Infranummulitic or, more commonly, directly onto the Upper Cretaceous (e.g., Lickorish and Ford, 1998). Despite its name, the unit contains siliciclastic detritus. The facies succession indicates progressive deepening of the basin. The base is usually characterized by a lag deposit rich in pebbles commonly displaying *Gastrochaenolites* borings (Carbone et al., 1980; Gupta, 1997; Evans and Elliott, 1999; Gupta and Allen, 2000; Varrone and D'Atri, 2007). This initial transgressive ravinement surface is overlain by shallow-water limestones rich in nummulitids and, locally, in coralline algae (Ravenne et al., 1987; Sinclair et al., 1998; Varrone and D'Atri, 2007) (Fig. 1C). Further deepening of the depositional environment is testified by the transition toward deposits rich in orthophragminids large benthic foraminifera (LBF from here onward) and planktonic foraminifera (Fig. 1C). The top of the unit generally presents a drowning (maximum flooding) surface with reworked bioclasts and abundant authigenic minerals, which testifies to the demise of the carbonate factory (Sinclair et al., 1998).

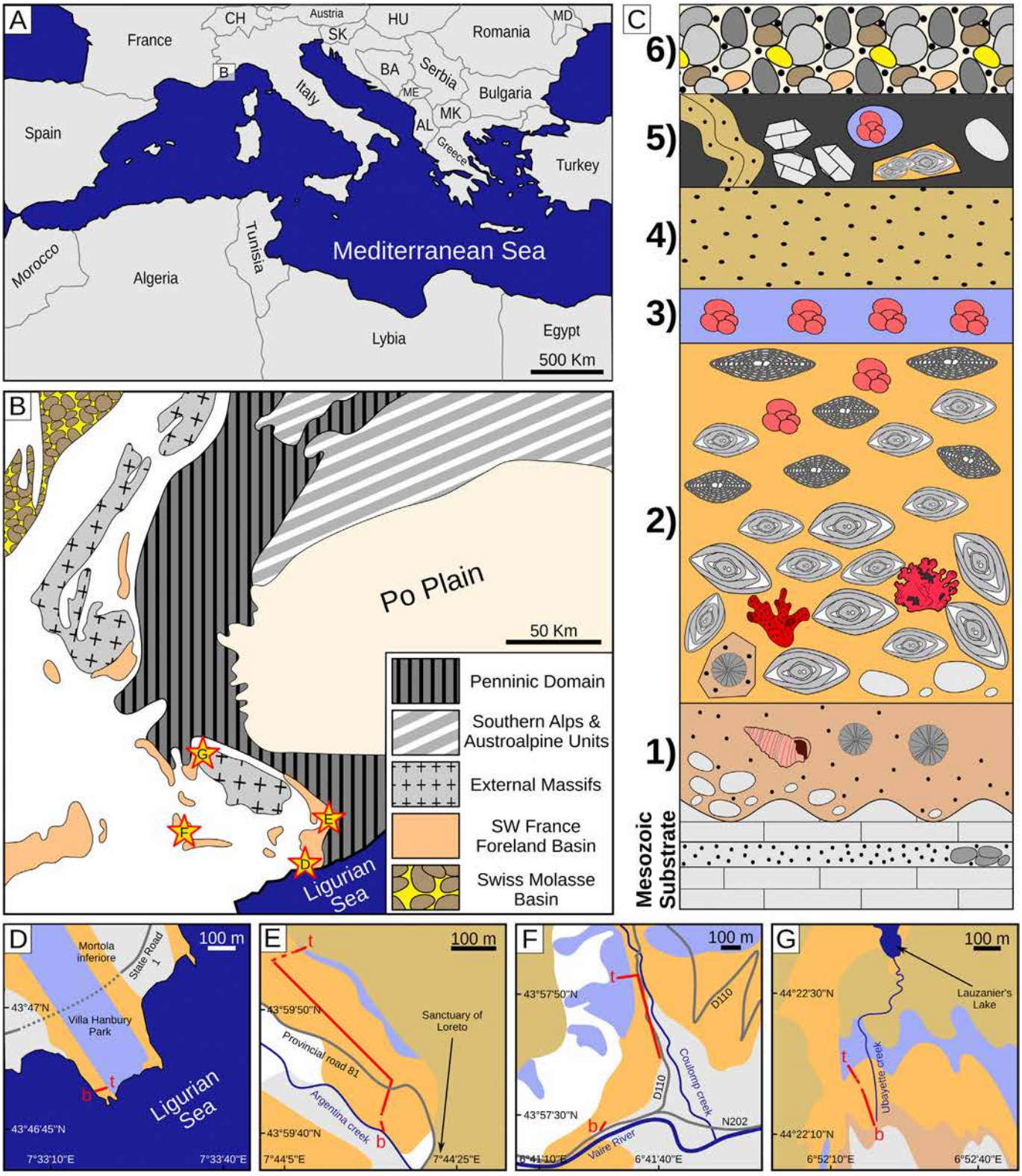

Fig. 1. Geographical and geological setting of the four investigated successions. A) Location of the study area within the Mediterranean region. B) Main geological units of NW Italy and SE France. C) Simplified stratigraphic log of the Western Alpine foreland basin; 1 = Infranummulitic; 2 = Nummulitic Limestone; 3 = Globigerina Marls; 4 = Sandstones; 5 = Mélanges; 6 = Molasse; symbols as in Fig. 3. Simplified geological maps of: D) Mortola section; key colors as in panel C; b, t = base and top of section; E) Loreto section; F) Braux section; G) Lauzanier section.

3) The overlying *Globigerina* Marls have a variable thickness ranging from few meters (Sturani, 1965; Barale et al., 2016) to 100–200 m (Allen et al., 1991; Sztrákos and Du Fornel, 2003). They deposited in a hemipelagic environment characterized by a limited clastic supply (Fig. 1C). The unit may be subdivided into a lower part (Blue Marls), mainly calcareous and containing coquina layers (sensu Schaffer, 1972) rich in reworked shallow-water bioclasts, and an upper part (Brown Marls) characterized by an increased

terrigenous fraction (Ravenne et al., 1987; Artoni and Meckel, 1998).

4) Heralded by the Brown Marls, siliciclastic supply culminates with the deposition of the Sandstones (locally called Grès d'Annot, Grès du Champsaur, Grès de Ville, Souloise Greywacke, or Ventimiglia Flysch) (Fig. 1C). This terrigenous unit is usually 500 to 1000 m thick (Ravenne et al., 1987; Ford et al., 1999; Sztrákos and Du Fornel, 2003; Mulder et al., 2010), but in the western stretches of the basin (Barrême area) is much thinner, around 50 m (Ford et al., 1999). Quartzo-feldspathic to litho-feldspatho-quartzose petrographic composition (Hu et al., submitted; classification after Garzanti, 2019b) and paleocurrents suggest that the main source of the detritus was located to the south and represented by the Sardinia–Corsica block and/or the Massif de l'Esterel (Ravenne et al., 1987; Lickorish and Ford, 1998; Ford et al., 1999; Mulder et al., 2010).
5) In the eastern part of the basin, the succession is sealed by the Mélange, which includes chaotic accumulation of detritus (300 to 600 m thick) from the internal Alpine domain (Ravenne et al., 1987; Evans and Elliott, 1999; Ford et al., 1999; Perotti et al., 2012; Maino and Seno, 2016) (Fig. 1C).
6) In the western part of the basin, instead, the succession is unconformably covered by the "Molasse". This name, once commonly used to define late orogenic clastic deposits accumulated in a foredeep basin (e.g., van Houten, 1973), is nowadays used in the Alpine region to indicate a widespread and thick unit consisting of clastic marine deposits accumulated in progressively shallower settings and finally overlain by fluvio-deltaic sediments (Evans and Elliott, 1999; Ford et al., 1999) (Fig. 1C).

2.2. Stratigraphic ages

The ages inferred for the Infranummulitic Formation (**1**), in the study area, should be comprised between the Lutetian (based on the presence of *Palaeotherium*; Sturani, 1965) and the Bartonian (based on gastropod and LBF assemblages; Sturani, 1965; Varrone and Clari, 2003; Sztrákos and Du Fornel, 2003). A Priabonian age has also been proposed by Sinclair et al. (1998) based on a different interpretation of the association of the vertebrates and gastropods reported by Sturani (1965). It must be noted that the limited knowledge of the distribution of Paleocene terrestrial vertebrates and marine gastropods species limits their stratigraphic significance. On the other hand, Varrone and Clari (2003) reported the presence of *Orbitolites* (whose extinction occur at the Bartonian/Priabonian boundary; Sartorio and Venturini, 1988; Serra-Kiel et al., 1998; Nebelsick et al., 2005; Boudaugher-Fadel, 2018), thus indicating a pre-Priabonian age for the Infranummulitic.

Because of the inherent difficulties in dating shallow-water limestones, the age of the Nummulitic Limestone (**2**) is also imprecisely constrained. The onset of deposition is diachronous, with the oldest strata exposed in the central Swiss Alps (Fliegenspitz beds, Thanetian age) (Ravenne et al., 1987; Ford et al., 1999; Allen et al., 2001; Kempf and Pfiffner, 2004). Within the study area, the base of the Nummulitic Limestone was constrained by LBF assemblages to the Bartonian (Sztrákos and Du Fornel, 2003; Varrone and Clari, 2003; Varrone and D'Atri, 2007), although ages ranging from late Lutetian to Priabonian have also been proposed (Bodelle, 1971; Campredon, 1977; Varrone and D'Atri, 2007). A general younging trend from SE to NW has also been documented (Campredon, 1977; Ford et al., 1999; Sztrákos and Du Fornel, 2003).

The overlying *Globigerina* Marls (**3**) are assigned, based on planktic foraminiferal and calcareous nannofossil assemblages, to the late Bartonian to early Priabonian in the eastern part of the study area, and to the Priabonian in the western part (Lickorish and Ford, 1998; Evans and Elliott, 1999; Sztrákos and Du Fornel, 2003; Varrone and D'Atri, 2007; Mulder et al., 2010).

According to calcareous nannofossils, planktonic foraminifera and reworked LBF, Sandstones (**4**) sedimentation in the study area should have started between the uppermost Bartonian and the Priabonian, while westward, in the Barrême area, it should have started during the Rupelian (Ford et al., 1999; Sztrákos and Du Fornel, 2003; Mulder et al., 2010). This is substantially consistent with the $^{40}Ar/^{39}Ar$ and K–Ar ages of the volcanic pebbles of the Sandstones that range between 35 and 30 Ma (Féraud et al., 1995; Montenat et al., 1999).

3. Material and methods

Four stratigraphic successions located in the area straddling the political border between NW Italy and SE France were accurately measured and sampled focusing on the Nummulitic Limestone and on immediately underlying and overlying intervals: Capo Mortola (NW Italy; 43°46′50.5″N 7°33′20.8″E), Loreto (NW Italy; 43°59′43.4″N 7°44′18.8″E), Braux (SE France; 43°57′31.3″N 6°41′36.9″E), and Lauzanier (SE France; 44°22′55.1″N 6°52′18.7″E) (Fig. 1B, D–G). Strata were logged in detail in the field, giving particular attention to major surfaces, macrofossil distribution, and sedimentary structures. The Capo Mortola section follows the section measured and sampled by Carbone et al. (1980). The investigated carbonate rocks were classified based on Dunham's (1962) classification, expanded by Embry and Klovan (1971) and refined by Lokier and Al Junaibi (2016). Representative rock samples were taken for petrographic and paleontological analyses. Wherever possible, further samples of isolated LBF were collected for biostratigraphic analysis. A total of 147 thin sections were analyzed (102 for skeletal assemblages, 25 dedicated to oriented sections of LBF, and 20 from units below and above the Nummulitic Limestone). Isolated LBF specimens were embedded in epoxy resin within a pill blister and abraded with silicon carbide to expose their equatorial plane (Coletti et al., 2019a). Subsequently, the specimens were prepared into thin sections. The taxonomy used for the classification of isolated orthophragminid specimens follows Less (1987). Skeletal assemblages and petrographic characteristics (including the amount of terrigenous material) were investigated by counting 350 points on each section and using a 250 μm mesh (Flügel, 2010). Full results of point-count analyses are included in Supplementary Table 1.

Paleoenvironmental interpretation was based principally on foraminiferal assemblages. In each section, all LBF were identified at the lowest possible taxonomic level and counted; small miliolids and planktonic foraminifera were also counted. The orthophragminid/nummulitid ratio (O/N), the large rotaliid/miliolid ratio, and the abundance of planktonic foraminifera were thus obtained for each sample. These parameters are depth-related and generally increase with increasing water depth (Hallock and Glenn, 1986; Ćosović et al., 2004; Beavington-Penney and Racey, 2004).

The terrigenous fraction was further investigated by powder X-ray diffraction (PXRD) on 32 bulk samples from different microfacies, and from units underlying and overlying the Nummulitic Limestone. The samples were initially ground in an agate mortar. PXRD analysis was performed on zero-background silicon plates with a Philips PW1140 diffractometer equipped with CoKα radiation (Kα1 wavelength 1.789 Å) operating at 40 kV and 20 mA. The samples were scanned between 3° and 70° 2θ with a step size of 0.02° 2θ and an acquisition time of 1 s per step. Data treatment was carried out with Panalytical X'pert HighScore Plus to identify the main mineralogical phases and a semi-quantitative analysis was carried out using the Reference Intensity Ratio (RIR) method (Chung, 1974).

4. Results

Based on the analysis of the skeletal and foraminiferal assemblages of the investigated sections, six main biofacies have been recognized:

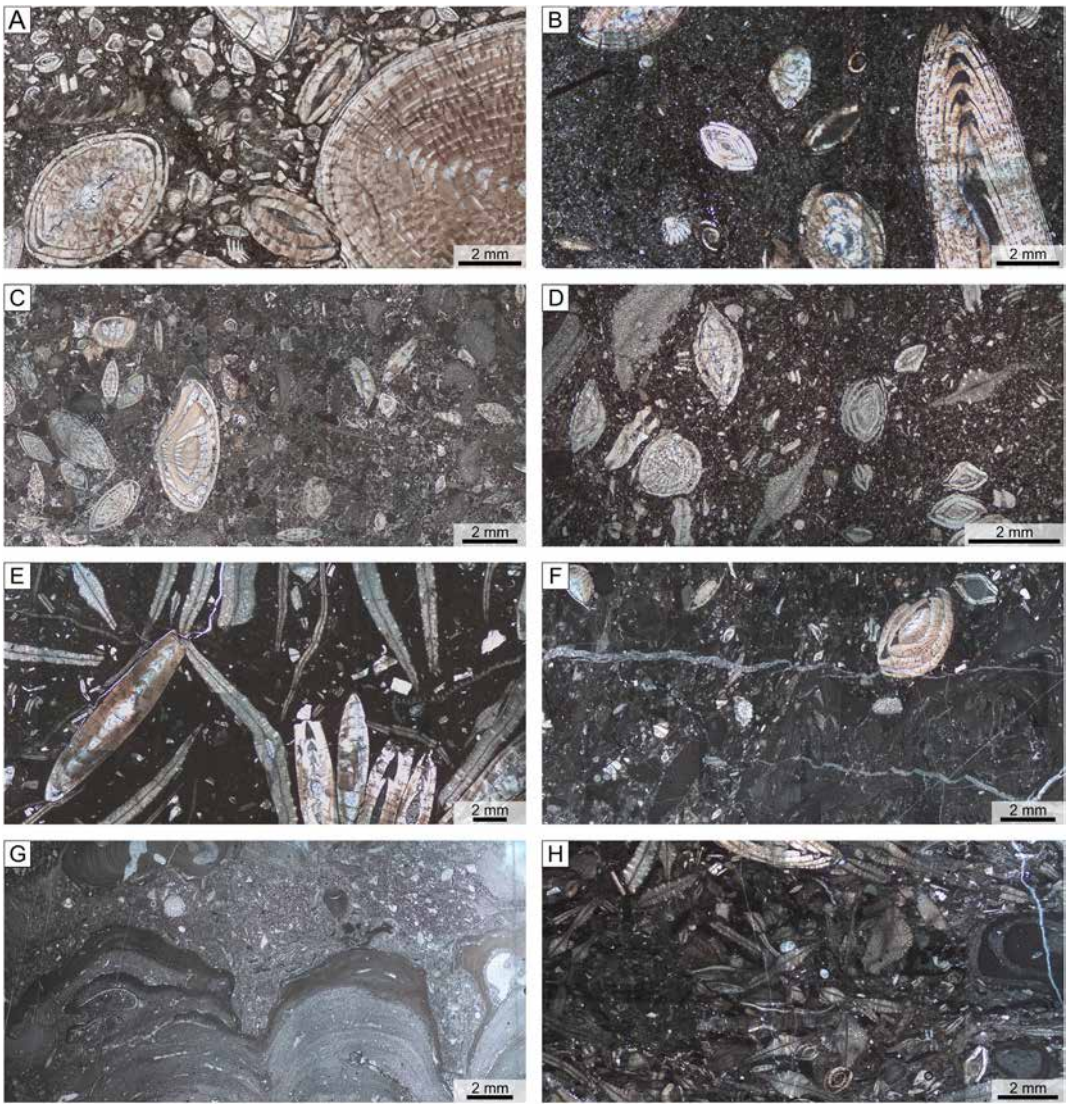

Fig. 2. Overview of the main recognized biofacies of the Nummulitic Limestone. A) Nummulitid biofacies, Capo Mortola; B) *Orbitolites*-bearing nummulitid biofacies, Capo Mortola; C) acervulinid-bearing nummulitid biofacies, Braux; D) nummulitid and orthophragminid biofacies, Braux; E) orthophragminid biofacies, Capo Mortola; F) coralline algal branches and LBF biofacies, Loreto; G) acervulinid and coralline algal biofacies, Loreto; H) orthophragminid and coralline algal biofacies; Loreto.

i) Nummulitid biofacies, occurring at the base of Mortola and Braux successions and characterizing the whole Lauzanier section. The skeletal assemblage is largely dominated by nummulitids (Fig. 2A); echinoderms and mollusks are usually common; solitary corals can be relevant. The foraminiferal assemblage is almost entirely consisting of benthic taxa and is dominated by the genus *Nummulites*; *Amphistegina* and small miliolids can be also common; planktonic foraminifera are very rare or absent. The nummulitid biofacies can be further subdivided into the *Orbitolites*-bearing nummulitid biofacies (lowermost Mortola section; Fig. 2B) and the acervulinid-bearing nummulitid biofacies (lowermost Braux section; Fig. 2C).

ii) Nummulitid and orthophragminid biofacies, occurring above the nummulitid biofacies in both the Mortola and Braux sections. It is dominated by LBF (Fig. 2D), associated with common mollusks and echinoderms, and rare serpulids (mainly *Ditrupa*); solitary corals can be abundant. Nummulitids (*Nummulites*, *Assilina*, *Operculina*) and orthophragminids dominate the foraminiferal assemblage; *Amphistegina* is rare, while planktonic foraminifera can be common.

iii) Orthophragminid biofacies, occurring above the nummulitid and orthophragminid biofacies in both the Mortola and Braux sections. The skeletal assemblage is almost entirely consisting of orthophragminids and planktonic foraminifera (Fig. 2E). *Assilina*, *Operculina*, and rare *Nummulites* also occur (Fig. 2E).

iv) Coralline algal branches and LBF biofacies, occurring in the Loreto section. Its skeletal assemblage consists of red calcareous algae (mainly pebble to granule-sized branches and rhodoliths) and LBF, associated with echinoderms, bryozoans and mollusks (Fig. 2F). The foraminiferal assemblage includes acervulinids, nummulitids, orthophragminids, small rotaliids, and small miliolids.

v) Acervulinid and coralline algal biofacies, occurring in the Loreto section. It is characterized by pebble-sized macroids (i.e. coated grains created by the concentric growth of encrusting organisms) built by encrusting foraminifera and coralline algae (Fig. 2G). The macroids are associated with free-living LBF, echinoderms and mollusks. The foraminiferal assemblage is dominated by acervulinids, associated with *Nummulites*, orthophragminids, *Alveolina*, and small miliolids.

vi) Orthophragminid and coralline algal biofacies, occurring only in the uppermost part of the Loreto section. Differently from the orthophragminid biofacies of Mortola and Braux, it displays abundant coralline algae (Fig. 2H).

4.1. Mortola

In the Mortola section, the Nummulitic Limestone is roughly 55 m thick and overlies Upper Cretaceous pelagic marlstones (Fig. 1D). The contact is an erosive surface, punctuated by small traces of boring organisms (possibly endolithic bivalves), carved into the underlying marlstones and filled with the coarser-grained bioclastic material of the Nummulitic Limestone. The basal layers of the Nummulitic Limestone contain common pebbles of dark chert, which do not occur up-section. Based on microfacies analysis, sedimentological features and macrofossil distribution, the measured section can be subdivided into five intervals (Figs. 3, 4).

Interval M1 (~17 m; *Orbitolites* bearing nummulitid biofacies). It consists of nummulitic rudstone layers (mainly lentil-sized megalospheric forms, associated with rarer microspheric forms with diameter up to 5 cm) alternating with packstone layers with rare large oyster and charcoal fragments (Fig. 4B, C). These are overlain by a floatstone layer (packstone matrix), where nummulitids, locally concentrated in lenses, are associated with solitary corals, mollusks (mainly large specimens of *Pycnodonte*, but also cardiidae, pectinids, gastropods, and vermetid gastropods; Fig. 4D, E), serpulids, rare echinoderms, and very rare colonial corals (Fig. 4F). Small burrows lined with nummulitid tests also occur (Fig. 4G). Microfacies analysis indicates that the skeletal assemblage is overwhelmingly dominated by LBF, associated with, in decreasing order of abundance, echinoderms (mainly irregular echinoids), small benthic foraminifera, serpulids (mainly *Ditrupa*), and mollusks (Fig. 5A–G; Table 1). The benthic foraminiferal assemblage is dominated by *Nummulites* (Fig. 5A, B) with common *Orbitolites* (both whole specimens and fragments; Fig. 5A, C), *Amphistegina* (Fig. 5F), small rotaliids and small miliolids (Fig. 5G). The terrigenous fraction accounts for up to 50% of the rock (Fig. 3; Table 1) and is mainly represented by fine-sand-sized angular quartz grains, plagioclase and

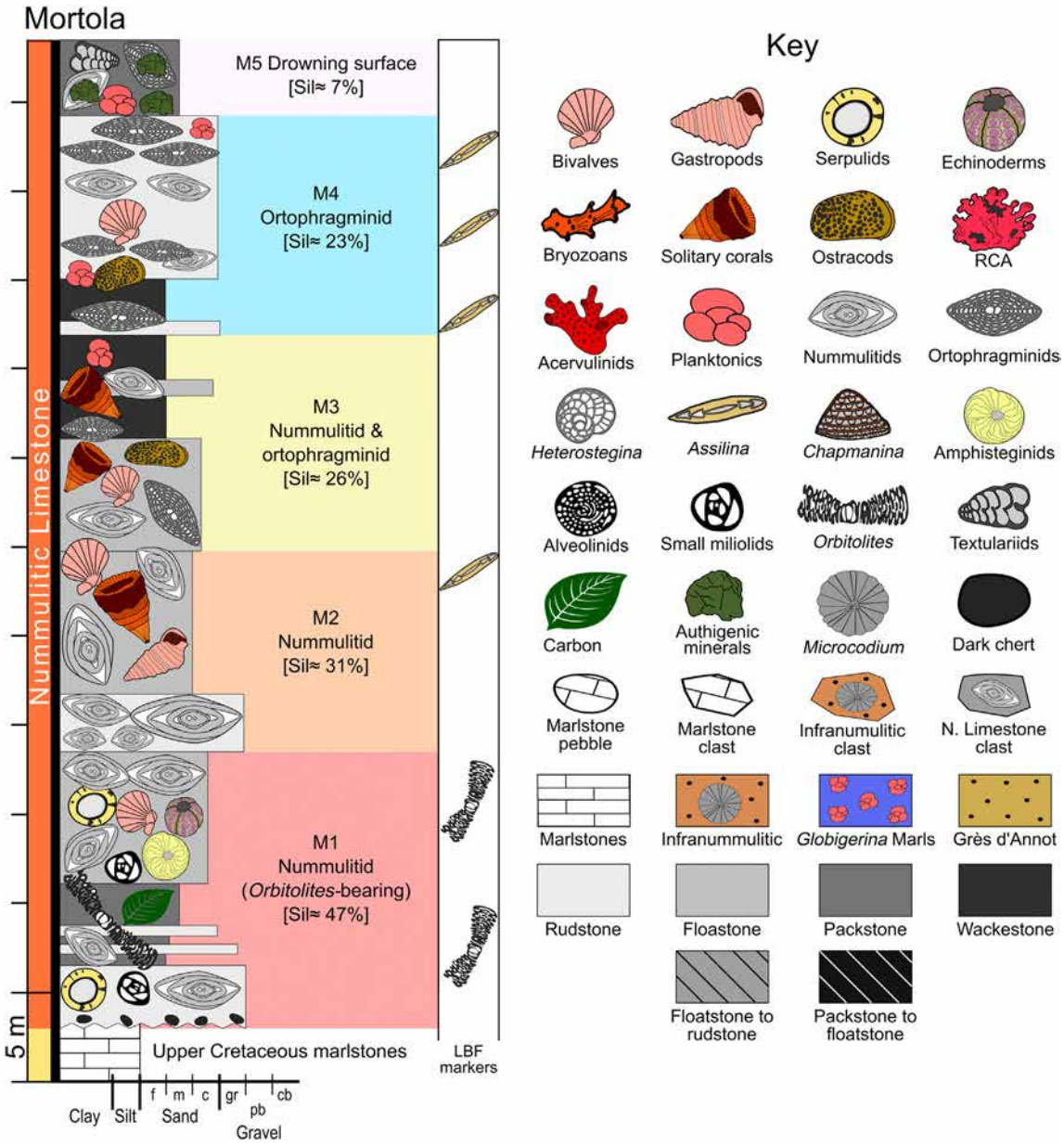

Fig. 3. Stratigraphic log of Mortola section with information on skeletal assemblages, average grain-size, and key to symbols. Sil = siliciclastic fraction; sub. = subfacies; LBF = large benthic foraminifera; RCA = coralline algae; f = fine; m = medium; c = coarse; gr = granules; pb = pebbles; cb = cobbles.

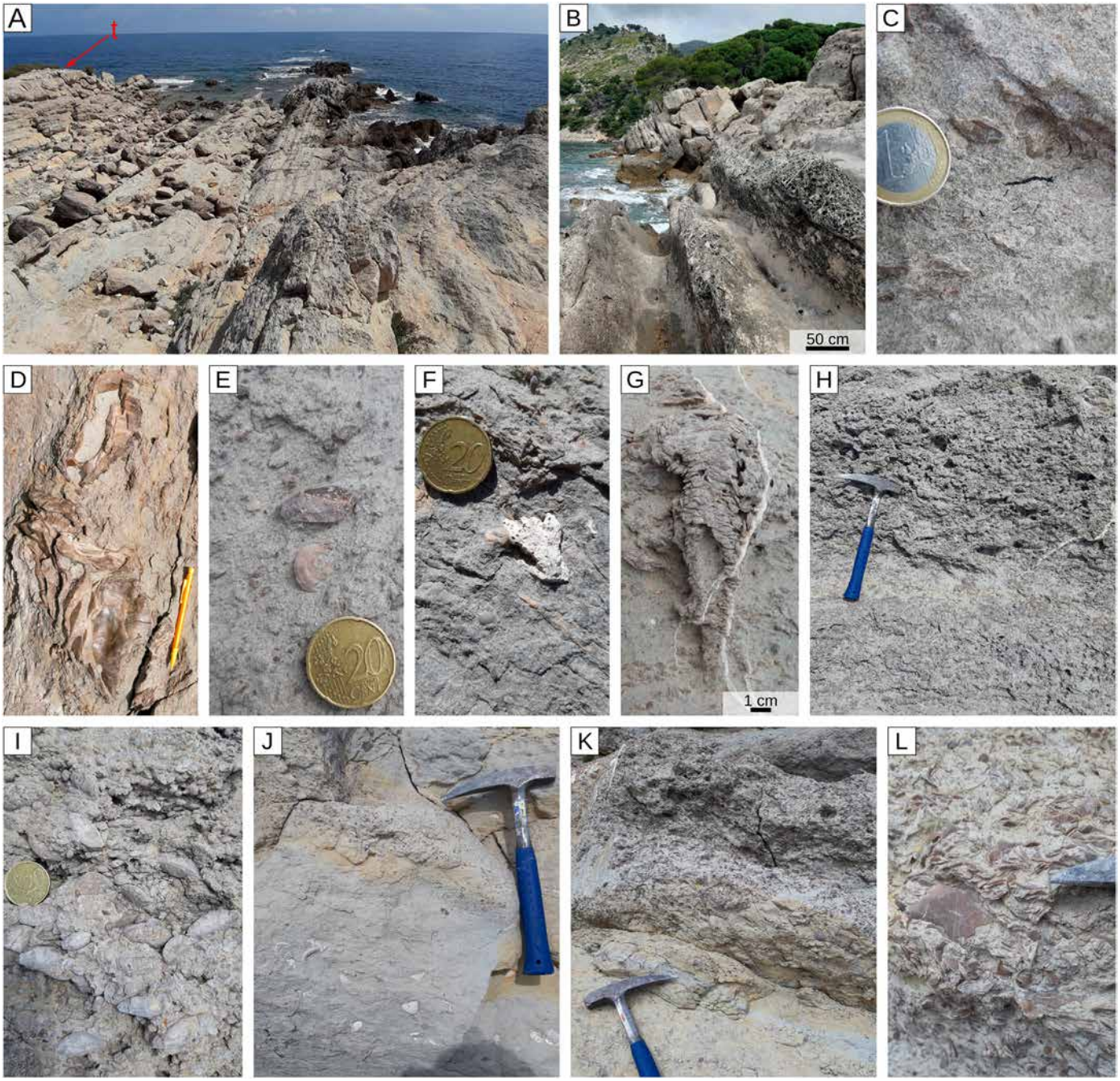

Fig. 4. Mortola section. A) Outcrop overview (base of section to the right, top to the left). B) M1, nummulitid rudstone alternating with fine-grained packstones; C) M1, charcoal fragment; D) M1, large *Pycnodonte* oysters; E) M1, vermetid gastropods; F) M1, colonial coral; G) M1, burrow lined with *Nummulites* tests; H) base of M2; I) M2, large-sized *Nummulites*; J) upper part of M2. K) Overview of M4; L) M4, thin and saddle-shaped orthophragminids with a large-sized microspheric specimen.

K-feldspar. The sparse heavy-mineral fraction chiefly consists of commonly euhedral zircon, tourmaline and rutile, with minor hornblende, staurolite, and garnet.

Interval M2 (~12 m; nummulitid biofacies). This interval starts with a 4 m-thick, nummulitic rudstone characterized by very common, thick megalospheric specimens associated with rarer gigantic microspheric specimens (diameter up to 5 cm; Fig. 4H, I), overlain by a 8 m-thick floatstone with a wackestone matrix displaying common nummulitids, solitary corals (Fig. 4J), gastropods, bivalves (mainly large *Pycnodonte* specimens and pectinids), scaphopods, rare serpulids, echinoderms (both spines and complete tests), and crab remains. Thin section analyses indicate that the skeletal assemblage is dominated by nummulitids (*Nummulites* and subordinate *Assilina*) with solitary corals, mollusks, small benthic foraminifera, echinoderms, serpulids, planktonic foraminifera, and ostracods (Table 1). Terrigenous grains represent ~30% of the rock and mainly consist of fine-sand-sized angular quartz grains, plagioclase, K-feldspar, and rare muscovite (Fig. 3; Table 1).

Interval M3 (~12 m; nummulitid and orthophragminid biofacies). Floatstone (with a wackestone matrix) with nummulitids (mainly small specimens with diameter <1 cm), solitary corals, *Pycnodonte* (commonly occurring in groups of several specimens attached together), and gastropods, alternating with wackestones almost devoid of macrofossils. The skeletal assemblage is dominated by LBF, associated with solitary corals, mollusks, small benthic foraminifera, echinoderms, planktonic foraminifera, serpulids, and ostracods (Fig.

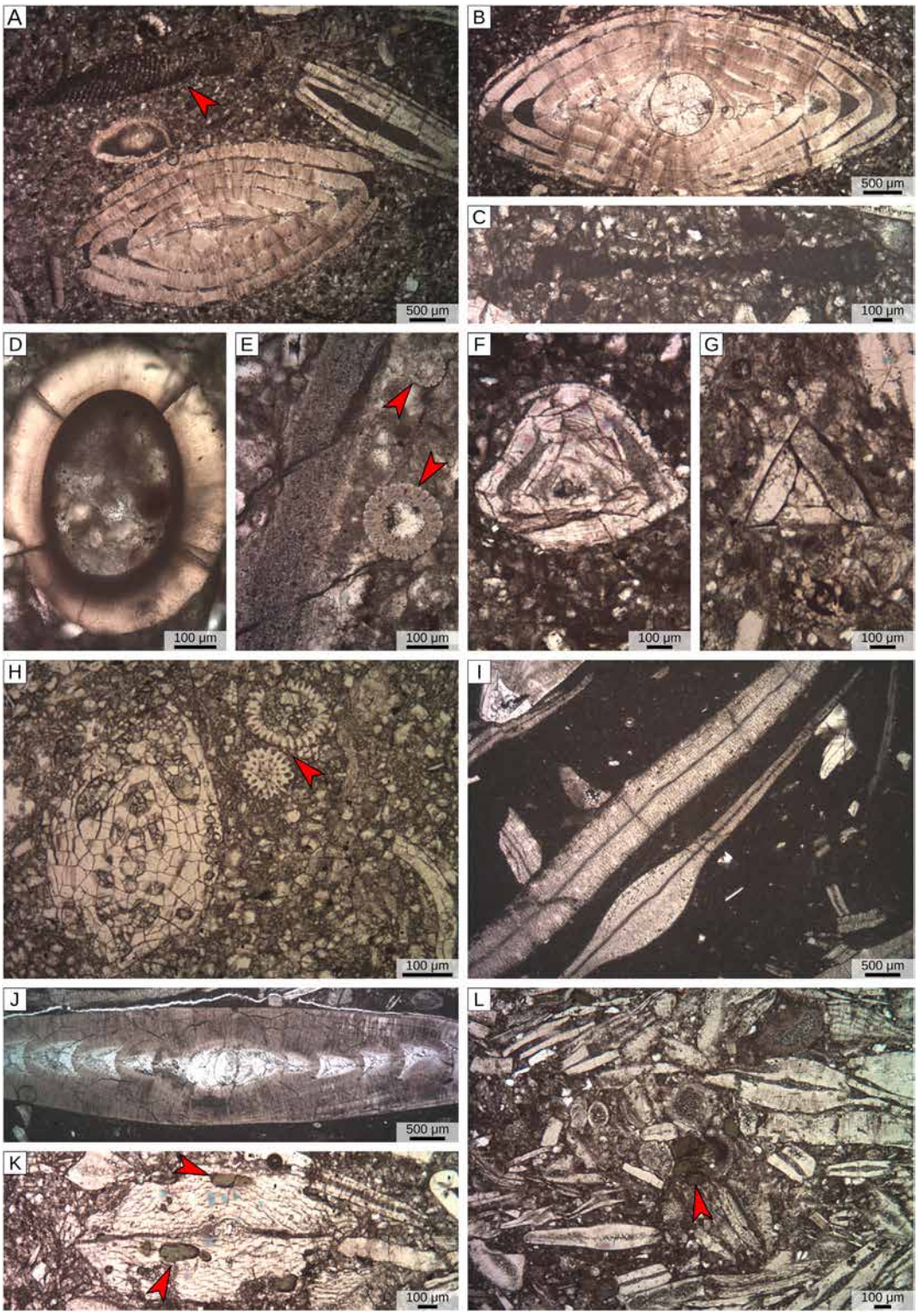

Fig. 5. Skeletal assemblage and microfossils in the Mortola section. A) M1, *Orbitolites* (red arrow) bearing nummulitid biofacies; B) M1, *Nummulites*, axial section; C) M1, *Orbitolites*, axial section; D) M1, *Ditrupa*; E) M1, echinoderm fragments (red arrow points at spines of irregular echinoids); F) M1. *Amphistegina*; G) M1, *Triloculina*; H) M3, *Lenticulina* and planktonic forams (red arrow); I) M4, thin and flat orthophragminids; J) M4, *Assilina*; K) M4, glaucony-filled orthophragminid; L) M5, well-sorted and fragmented foraminifera (red arrow points at glaucony). (For interpretation of the references to color in this figure legend, the reader is referred to the web version of this article.)

5H; Table 1). The benthic foraminiferal assemblage is dominated by orthophragminids, *Nummulites* and small rotaliids including *Lenticulina*. The detrital fraction accounts for roughly 25% of the rock and mainly consists of coarse-silt-sized angular quartz grains, K-feldspar, plagioclase and rare muscovite (Fig. 3; Table 1).

Interval M4 (~13 m; orthophragminid biofacies). The base of this interval consists of a rudstone, with a wackestone matrix, rich of flat and thin nummulitids (mainly *Assilina exponens*), and orthophragminids including microspheric specimens up to several cm in diameter (Fig. 4K). This rudstone is overlain by a 50 cm-

Table 1
Skeletal composition, foraminiferal assemblage and characteristics of the terrigenous fraction for each biofacies identified in the Nummulitic Limestone. A = absent; RR = very rare; R = rare; NC = not common; C = common; CC = very common; RCA = red calcareous algae; LBF = large benthic foraminifera; PXRD = powder X-ray diffraction.

Site	Mortola	Mortola	Mortola	Mortola	Loreto	Loreto	Loreto	Braux	Braux	Braux	Braux	Lauzanier
Biofacies	Nummulitid (*Orbitolites*-bearing)	Nummulitid	Nummulitid & ortophragminid	Ortophragminid	RCA branches & LBF	Acervulinid & RCA	Ortophragminid & RCA	Nummulitid (acervulinid-bearing)	Nummulitid & ortophragminid	Nummulitid & ortophragminid (mass transport)	Ortophragminid	Nummulitid
Skeletal assemblage [point counting]												
Coralline algae	0%	0%	0%	0%	68.5%	24.5%	30%	2%	0.1%	0.3%	0%	0%
Solitary corals	0%	18.5%	15%	0%	4%	0%	0%	0.4%	0.1%	3.5%	0%	7%
Benthic foraminifera	85%	71.5%	63%	93%	17.5%	67%	61%	81%	89%	78.5%	87%	74.5%
(nummulitids)	(66%)	(69%)	(37%)	(17%)	(4.5%)	(5.5%)	(11%)	(42%)	(58%)	(40.5%)	(5.5%)	(62%)
(orthophragminids)	(0%)	(0.5%)	(15%)	(71%)	(1.5%)	(2%)	(47.5%)	(0.5%)	(22%)	(21.5%)	(63.5%)	(5%)
(amphisteginids)	(4%)	(0%)	(0%)	(0%)	(0%)	(0.5%)	(0%)	(4.5%)	(0.5%)	(0%)	(0%)	(2%)
(large miliolids)	(7%)	(0%)	(0%)	(0%)	(0%)	(1.5%)	(0%)	(0.1%)	(0%)	(0%)	(0%)	(0%)
(small miliolids)	(3.5%)	(0%)	(0%)	(0%)	(1.5%)	(1.5%)	(0%)	(4.9%)	(0.3%)	(2.5%)	(0%)	(1.5%)
(small rotaliids)	(4.5%)	(2%)	(11%)	(5%)	(3%)	(2.5%)	(2%)	(11%)	(7%)	(8.5%)	(10%)	(3%)
(encrusting foraminifera)	(0%)	(0%)	(0%)	(0%)	(5%)	(50%)	(0.5%)	(14%)	(1%)	(0%)	(0%)	(0%)
Planktonic foraminifera	0%	0.5%	1%	5%	0%	0%	0%	0%	1.3%	2%	8%	0%
Echinoderms	9.4%	1.5%	2.5%	1%	4%	3.5%	2.5%	9%	5%	7.5%	3%	11.5%
Mollusks	1.5%	6%	16%	0%	1.5%	0.9%	4%	5.5%	2.5%	4%	0%	7%
Bryozoans	0%	0%	0%	0%	3.5%	0.1%	2%	1.5%	0.5%	0.2%	0%	0%
Serpulids	4%	0.5%	1%	0%	0.1%	3.5%	0%	0.2%	1%	2.5%	0%	0%
Others	0.1%	1.5%	1.5%	1%	0.4%	0.5%	0.5%	0.4%	0.5%	1.5%	2%	0%
Foraminiferal assemblage [area counting]												
Large rotaliid/miliolid (average)	10.65	57.25	n.a.	n.a.	2.47	4.61	136.77	9.54	23.91	10.69	79.75	17.24
Ortophragminid/nummulitid (average)	0.00	0.04	0.512	3.46	0.62	0.57	27.31	0.02	0.23	0.52	4.67	0.04
Amphistegina (average)	CC	NC	NC	A	NC	NC	A	CC	NC	R	A	C
Planktonic foraminifera (average)	RR	R	NC	C	RR	A	NC	A	NC	NC	C	A
Terrigenous fraction												
Siliciclastic minerals (PXRD)	47%	31%	26%	23%	2.5	1%	9%	4%	8.5%	8%	11%	16%
Dominant mineral (PXRD)	Quartz	Quartz	Quartz	Quartz	Quartz	Quartz	Quartz	Quartz	Quartz	Quartz	Quartz	Quartz
Terrigenous elements (point counting)	Quartz (CC), charcoal (R)	Quartz (CC)	Quartz (CC)	Quartz (CC)	//	//	//	Rock fragments (C); charcoal (NC)	Rock fragments (R); charcoal (R)	Rock fragments (C); charcoal (RR)	//	Quartz (CC)

thick wackestone layer and further overlain by a rudstone characterized by densely packed, thin, and saddle-shaped orthophragminids including microspheric specimens up to 5 cm in diameter (Fig. 4L). This layer also displays decimeter-long burrows lined by LBF. The skeletal assemblage almost entirely consists of LBF (orthophragminids and subordinate nummulitids), associated with planktonic foraminifera, small rotaliids (including *Lenticulina* and *Stilostomella*), echinoderms, and ostracods (Fig. 5I, J; Table 1). Coarse-silt-sized quartz grains represent the bulk of the terrigenous fraction, together with plagioclase, K-feldspar, and muscovite (Fig. 3; Table 1). Toward the top of the interval, foraminiferal chambers can be filled with glaucony (Fig. 5K).

Interval M5 (~1 m; drowning lag). The Nummulitic Limestone is capped by a drowning surface characterized by a well-sorted foraminiferal packstone containing mollusks, echinoderms, and glaucony commonly filling foraminiferal tests (Fig. 5L). The foraminiferal assemblage is dominated by nummulitids and orthophragminids, associated with common planktonic foraminifera, textulariids, small rotaliids (including *Lenticulina*), and rare miliolids. The minor siliciclastic fraction (Fig. 3) consists of fine-sand-sized angular quartz grains and includes a small heavy-mineral fraction displaying zircon, tourmaline, rutile, biotite, apatite, staurolite, and garnet.

4.2. Loreto

In the Loreto area (municipality of Triora; NW Italy; Fig. 1E), Upper Cretaceous pelagic marlstones are unconformably overlain by a 2 to 4 m-thick paraconglomerate comprising poorly sorted clasts of the marlstones and of the Nummulitic Limestone, together with loose Eocene bioclasts (mainly nummulitids and fragments of coralline algae) (Figs. 6, 7). The significant siliciclastic fraction, making up to ~30% of the rock, consists of coarse-silt-sized quartz grains with subordinate plagioclase, muscovite, and chlorite (Figs. 6, 7C). Angular and poorly sorted clasts of Nummulitic Limestone, ranging from granule to boulder-size (Fig. 7B, E, G), are mostly consisting of LBF (*Nummulites*, *Assilina*, orthophragminids, and *Sphaerogypsina*) and coralline algae. Rare fragments of encrusting acervulinids also occur. Coralline algae are poorly preserved and the few recognizable fragments belong to the genus *Sporolithon*. Most of the Nummulitic Limestone material recovered from the paraconglomerate displays *Microcodium*-like alteration (Fig. 7G). The overlying 140-m thick Nummulitic Limestone, based on microfacies analysis, sedimentological features and macrofossil distribution, can be divided into five intervals (Figs. 6, 8A).

Interval L1 (~35 m; coralline-algal branches and LBF biofacies). The basal interval consists of floatstones to rudstones (with packstone matrix) dominated by coralline algae and LBF, including large microspheric specimens of *Nummulites* up to several centimeters in diameter. Rare large specimens of *Pycnodonte* also occur (Fig. 8B). The skeletal assemblage includes coralline algae (mainly *Sporolithon*, associated with Hapalidiales and Corallinales), LBF, associated with encrusting acervulinids, small benthic foraminifera, echinoderms, bryozoans, and mollusks (Fig. 9A–D; Table 1). The benthic foraminiferal assemblage includes *Nummulites*, *Assilina*, orthophragminids, *Sphaerogypsina*, *Amphistegina*, small rotaliids, small miliolids and textulariids (Fig. 9B, C). The terrigenous fraction is minor and quartz-rich (Fig. 6; Table 1).

Interval L2 (~50 m; mass-transport deposits). Finely laminated, dark gray wackestones rich in organic matter, displaying dish structures related to dewatering, and characterized by fragmented and poorly preserved bioclasts, usually occurring in thin layers (1–2 cm) and displaying an imbricated fabric (Figs. 8C, 9E). Bioclasts include echinoderm fragments, planktonic foraminifera, coralline algae, LBF (*Nummulites*, *Assilina*, orthophragminids), small rotaliids (including *Lenticulina*), textulariids, ostracods, bivalves, and rare small miliolids. Most of bioclasts are poorly preserved and fragmented except planktonic foraminifera that are well preserved (Fig. 9F, G). Authigenic pyrite crystals may overgrow foraminiferal tests (Fig. 9H). The significant terrigenous fraction consists of coarse-silt-sized angular quartz grains together with chlorite, muscovite, and plagioclase (Fig. 6).

Interval L3 (~18 m; acervulinid and coralline algal biofacies). The central part of the section is characterized by dark-colored acervulinid macroid rudstones with a packstone matrix (Fig. 8D). Coralline algae commonly overgrow foraminiferal macroids.

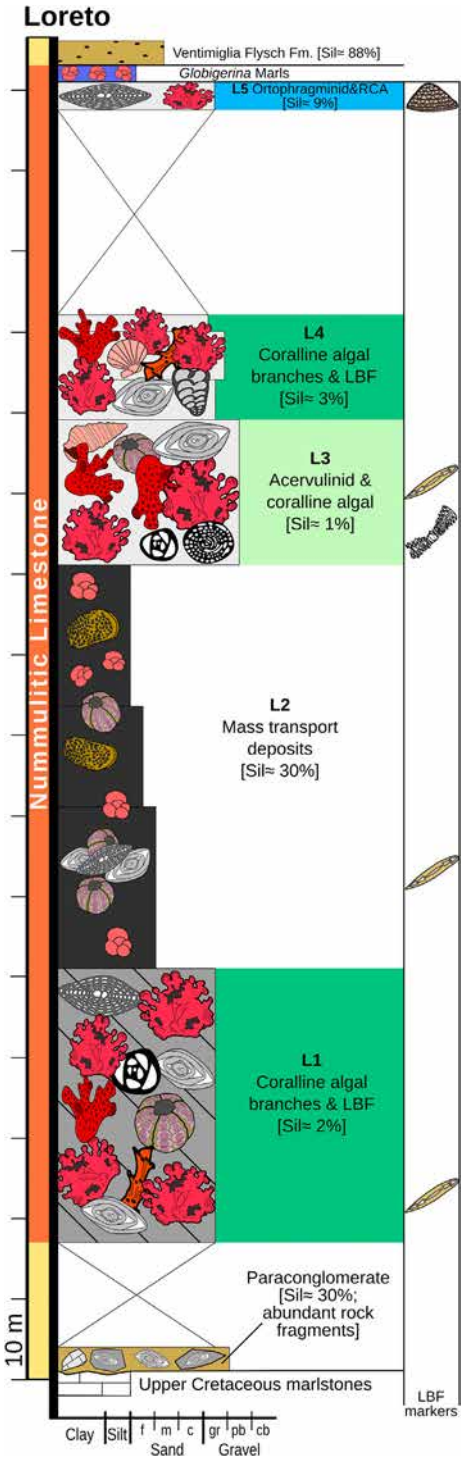

Fig. 6. Stratigraphic log of Loreto section with information on skeletal assemblage and average grain-size. Symbols and abbreviations as in Fig. 3.

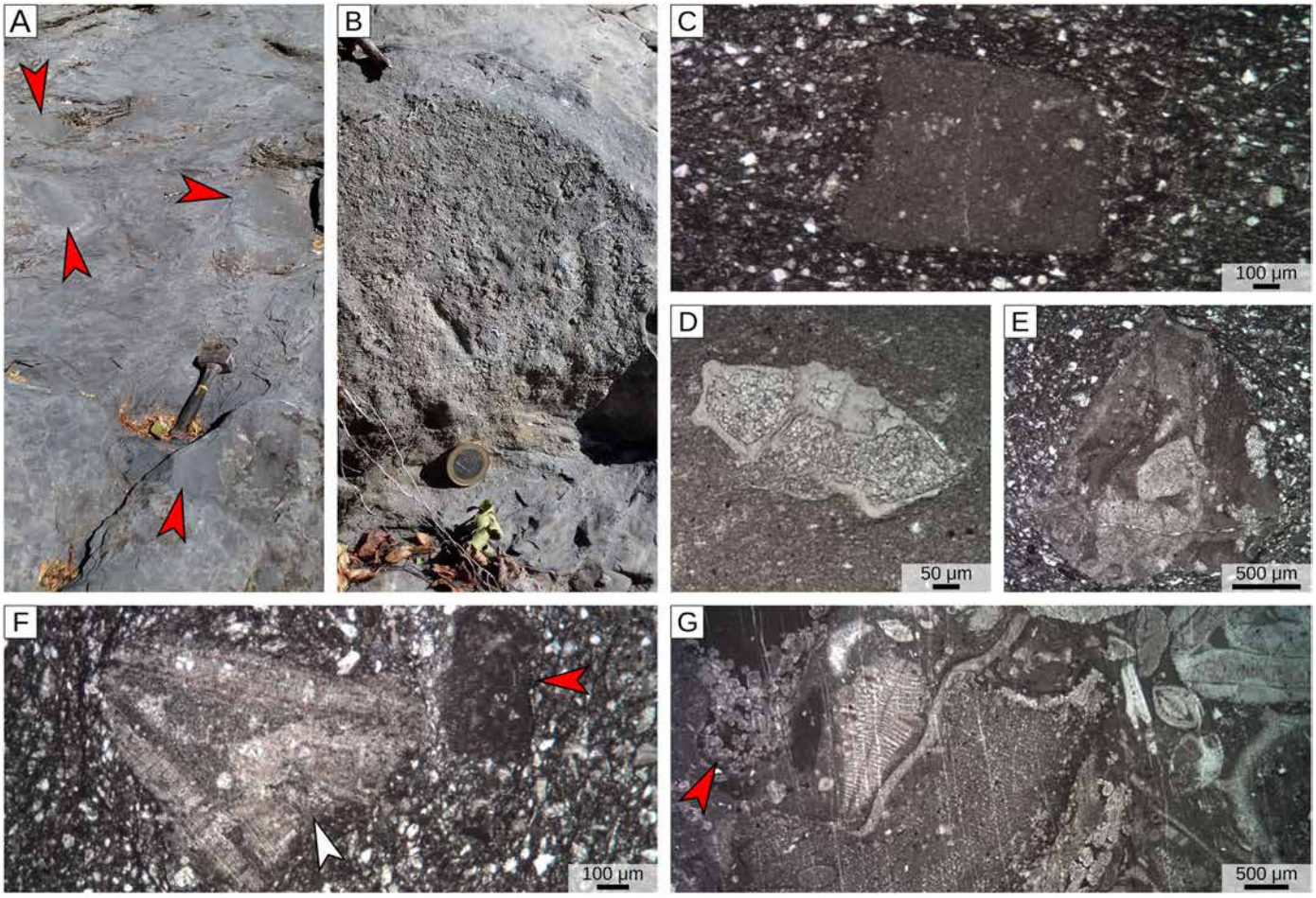

Fig. 7. Paracoglomerate at the base of the Loreto section. A) Outcrop view of the paraconglomerate (red arrow points at clasts of Upper Cretaceous pelagic marls). B) Clast of Nummulitic Limestone. C) Angular clast of Upper Cretaceous pelagic marls embedded in paraconglomerate matrix. D) Specimen of *Globotruncana* contained in a clast of Upper Cretaceous pelagic marlstones. E) Angular clast of Nummulitic Limestone. F) Paleogene bioclasts embedded in the paraconglomerate matrix (white arrow points at *Nummulites* fragment, red arrow points at coralline alga). G) Detail of skeletal assemblage contained in a clast of Nummulitic limestone (red arrow points at an altered coralline alga). (For interpretation of the references to color in this figure legend, the reader is referred to the web version of this article.)

Gastropods and LBF are common, and solitary corals are rare. The skeletal assemblage is dominated by encrusting acervulinids and coralline algae, associated with LBF, small benthic foraminifera, echinoderms, and encrusting serpulids (Fig. 9I–L; Table 1). Green calcareous algae, bryozoans, mollusks, and ostracods are rare. Benthic foraminifera include common *Nummulites* and *Sphaerogypsina* associated with *Alveolina*, *Amphistegina*, *Eorupertia*, small rotaliids, small milioliids, textulariids, and rare *Orbitolites* and *Assilina* (Fig. 9J–L). Coralline algal assemblage is dominated by *Sporolithon* associated with Hapalidiales and Corallinales (including *Lithoporella*). The terrigenous fraction is negligible.

Interval L4 (up to 35 m-thick; coralline-algal branch and LBF biofacies). The upper part of the Loreto cliff is characterized by dark-colored massive rudstones with a packstone matrix. Since the cliff is vertical, only the lower portion of this interval was extensively investigated. Coralline algae are slightly less abundant than in the L1 interval, while LBF and solitary corals are slightly more common. The foraminiferal assemblage is also similar and the most noticeable difference is the lack of *Assilina*.

Interval L5 (3 m; orthophragminid and coralline algal biofacies). Only observable at the top of the cliff (Fig. 8A). It consists of a few meters of dark-gray rudstones with a packstone matrix dominated by thin and flat orthophragminids, whose abundance notably increases upsection, coralline algae (including *Sporolithon* and Hapalidiales), associated with thin and flat nummulitids, mollusks, echinoderms, small benthic foraminifera, bryozoans, planktonic foraminifera and acervulinids (Fig. 9M; Table 1). The benthic foraminiferal assemblage mostly consists of orthophragminids, *Nummulites*, small rotaliids, textulariids, *Chapmanina*, *Sphaerogypsina* (Fig. 9N), and rare small miliolids. Quartz, muscovite, and plagioclase occur (Fig. 6; Table 1).

The Nummulitic Limestone is overlain by a thin layer of laminated *Globigerina* Marls, rich of sand-sized angular quartz grains and planktonic foraminifera, which is in turn overlain by the Ventimiglia Flysch (Figs. 8E, 9O). These fine-grained sandstones contain quartz and abundant plagioclase with common micas (chlorite, biotite, muscovite) associated with a sizable heavy mineral faction including zircon, apatite, titanium oxides, tourmaline and hornblende (Figs. 6, 9P).

4.3. Braux

In the Annot area, the Nummulitic Limestone is generally underlain by the Infranummulitic. However, in the Braux section, the 35 m-thick Nummulitic Limestone directly overlies Upper Cretaceous marlstones (Figs. 1F, 10, 11A). The limestone can be subdivided into four intervals (Fig. 10).

Interval B1 (~13 m; acervulinid-bearing nummulitid biofacies). The lowermost interval of the section consists of layers of rudstones several meters thick (Fig. 11A). The skeletal assemblage is dominated by nummulitids that occur as lentil-sized megalospheric specimens and rare microspheric specimens with a diameter of ~1 cm (Fig. 12A;

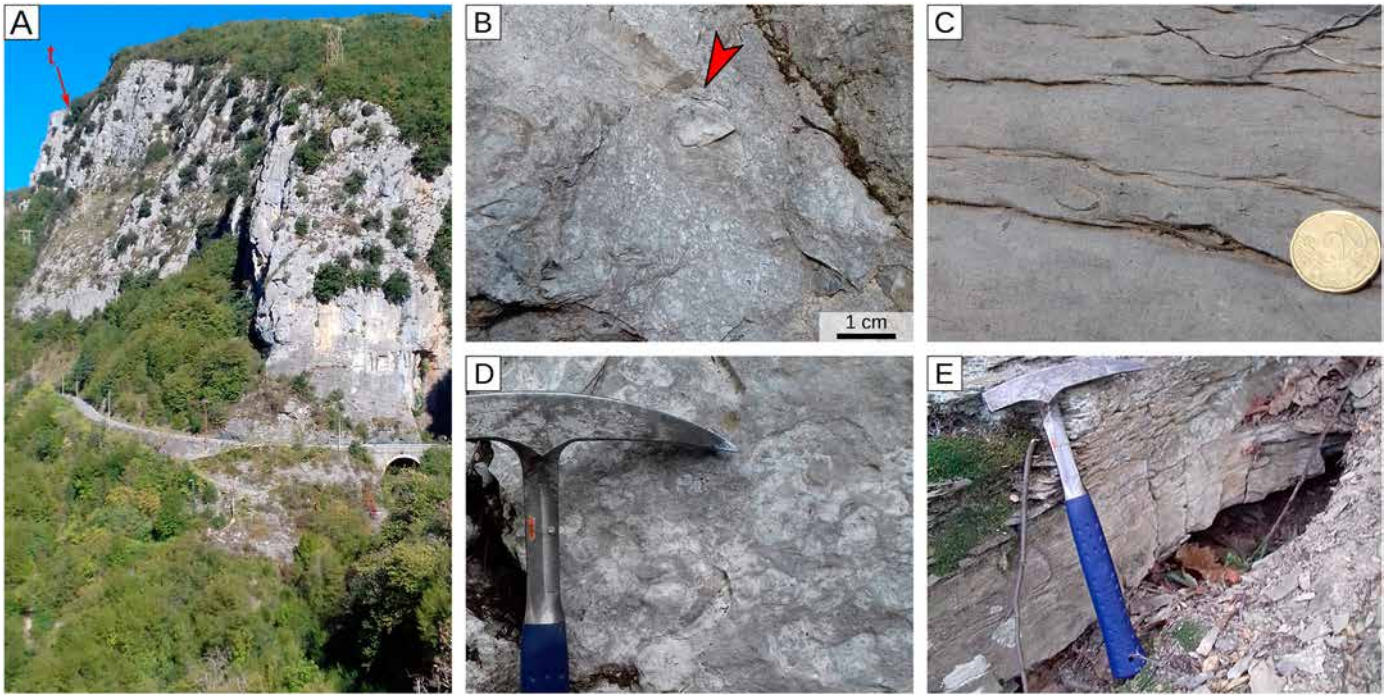

Fig. 8. Loreto section. A) Outcrop overview (t = top of section); B) L1, *Pycnodonte* shell (red arrow); C) L2, dish structures; D) L3, overview of the acervulinids and coralline algal biofacies characterized by abundant acervulinid macroids; E) Ventimiglia Flysch Fm. (For interpretation of the references to color in this figure legend, the reader is referred to the web version of this article.)

Table 1). Gigantic specimens (up to 3 cm in diameter) were observed only at the very base of the interval (Fig. 11B). Encrusting acervulinids are common and mainly occur as small nodules (≤1 cm in diameter), usually with a hooked morphology (Fig. 12B, C). Other bioclasts include small benthic foraminifera, echinoderms (locally as large test fragments), mollusks, coralline algae (small nodules of *Sporolithon* and articulated Corallinales), bryozoans, solitary corals, green calcareous algae, and serpulids (both encrusting taxa and free-living ones like *Ditrupa*) (Fig. 12D, E). The benthic foraminiferal assemblage includes common *Nummulites*, *Amphistegina*, *Chapmanina*, *Eorupertia*, *Triloculina*, *Quinqueloculina*, and small rotaliids; textulariids and orthophragminids are rare (Fig. 12F–J). Rock fragments eroded from the Upper Cretaceous pelagic marlstones and the *Microcodium*-bearing Infranummulitic deposits are significant (Fig. 12A). Small charcoal fragments were frequently observed (Fig. 11C). Quartz grains represent ~4% of the rock (Fig. 10; Table 1).

Interval B2 (~11 m; nummulitid and orthophragminid biofacies). Packstones to floatstones dominated by LBF, associated with small benthic foraminifera, echinoderms, encrusting acervulinids, mollusks (mainly *Pycnodonte*), planktonic foraminifera, rare bryozoans, serpulids (mainly *Ditrupa*), solitary corals, coralline algae, and ostracods (Fig. 12K, L; Table 1). Benthic foraminifera are mostly nummulitids (both *Operculina* and *Nummulites*), associated with orthophragminids, small rotaliids, rare *Amphistegina*, and small miliolids (Fig. 12M). The terrigenous fraction consists of fine-sand-sized quartz grains and rare rock and charcoal fragments (Fig. 10; Table 1).

Interval B3 (~10 m; mass transport deposits; nummulitid and orthophragminid biofacies). The third interval of Braux section is separated from the underlying one by a markedly erosive surface (Fig. 11D). It consists of irregularly bedded packstones and floatstones (with a packstone matrix) and displays channelized features (Fig. 11D, E). Packstone layers mostly consist of comminuted bioclasts, while floatstone layers are usually characterized by coarse-grained bioclasts with an imbricated fabric (Fig. 12N). The skeletal assemblage is dominated by LBF associated with small benthic foraminifera, echinoderms, mollusks, and solitary corals, *Ditrupa*, ostracods, and bryozoans. Rare coralline algae only occur in floatstone layers with imbricated bioclasts. Planktonic foraminifera are common in packstone layers (Table 1). *Nummulites*, *Operculina*, orthophragminids and small rotaliids (including *Lenticulina*) dominate the benthic foraminiferal assemblage. Small miliolids are locally common, and textulariids are rare. *Amphistegina* and *Chapmanina* occur in floatstone layers. The terrigenous fraction mainly consists of coarse-silt-sized quartz grains (Fig. 10; Table 1). Rock fragments derived from Infranummulitic lithologies and Upper Cretaceous marlstones occur in the floatstone layers (Fig. 12N).

Interval B4 (~2 m; orthophragminids biofacies). Poorly-lithified floatstone with a wackestone matrix, displaying a diversified orthophragminid assemblage (including *Discocyclina dispansa dispansa* and other discocyclinids), with subordinate nummulitids (*Nummulites*, *Operculina*, and *Heterostegina*), small benthic (*Lenticulina*, *Cibicides*, rare *Textulariids*, very rare *miliolids*) and planktonic foraminifera, rare echinoderms and ostracods (Figs. 11F, 13; Table 1). The quartzose terrigenous fraction represents ~11% of the rock (Fig. 10; Table 1).

The base of the overlying *Globigerina* Marls contains a resedimented layer of well-sorted fine-grained grainstone dominated by comminuted bioclasts including nummulitids and orthophragminids, rich in marly intraclasts, and with a significant terrigenous fraction (Fig. 11G). The *Globigerina* Marls are overlain by the Grès d'Annot (Fig. 11H).

4.4. Lauzanier

In the Lauzanier valley, located in the Argentera Massif (Fig. 1G), the Upper Cretaceous and the Nummulitic Limestone are separated by the Infranummulitic (Figs. 14, 15A, B), which displays a remarkable facies variability and includes several distinct lithofacies: 1) *Microcodium*-bearing conglomerates with clasts derived from the Upper Cretaceous pelagic marlstones (ranging in thickness between

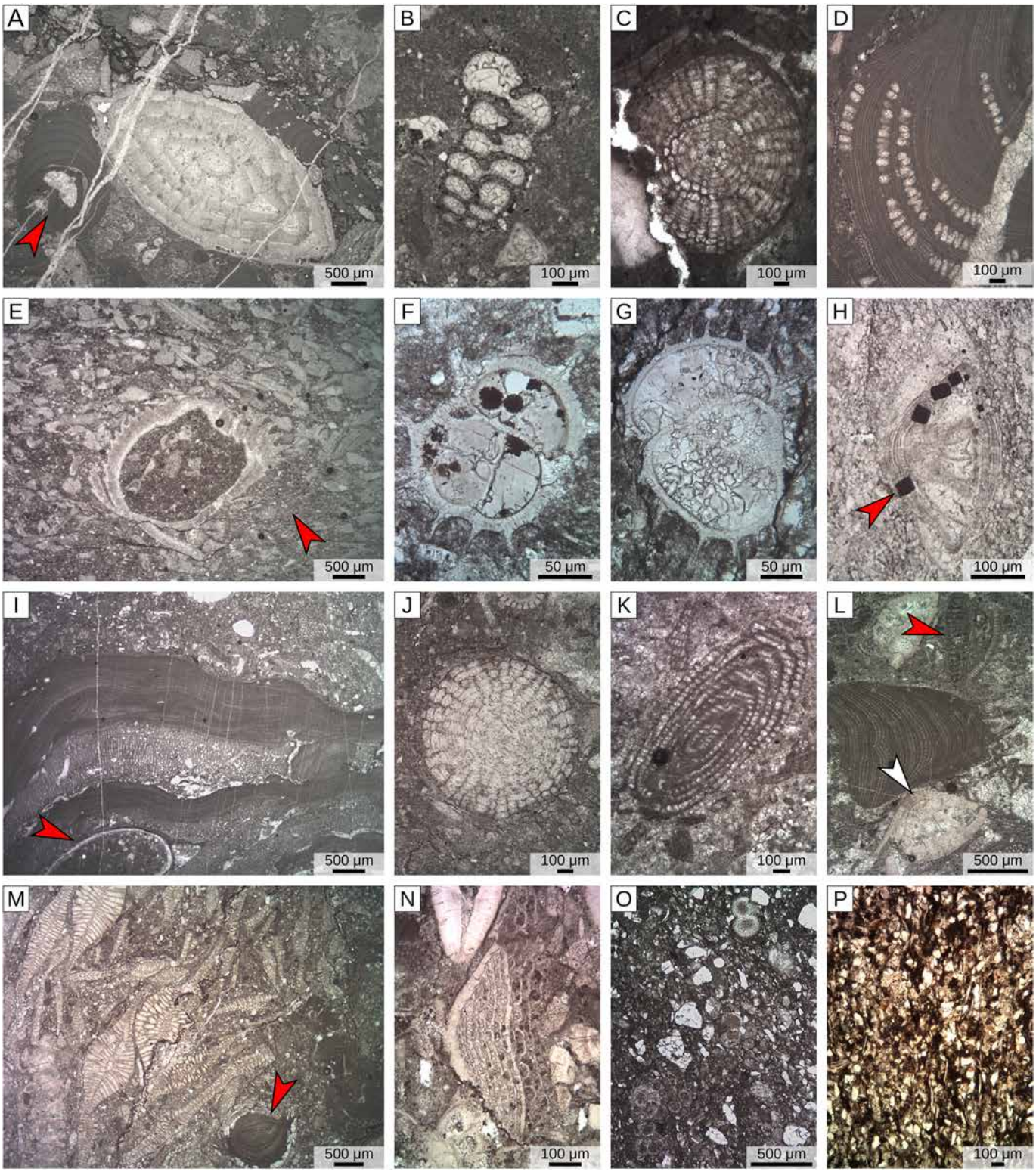

Fig. 9. Skeletal assemblage and microfossils in the Loreto section; A) L1, coralline algal branches and LBF biofacies, corallinales = red arrow; B) L1, textulariid; C) L1; *Sphaerogypsina*; D) L1; *Sporolithon*; E) L2, imbricated fabric, the red arrow points at a bioclast-free area on the protected lee side of a large bioclast; F, G) L2, well preserved planktonic foraminifera (possibly *Acarina*); H) L2, benthic foraminifera with authigenic pyrite growing from wall of chambers; I) L3, coralline algae and acervulinids growing together (red arrow points at encrusting serpulids); J) L3, *Sphaerogypsina*; K) L3, *Alveolina*; L) L3, *Amphistegina* (white arrow) and *Orbitolites* fragment (red arrow); M) L5, coralline algal fragment (red arrow); N) L5, *Chapmanina*. O) *Globigerina* Marls. P) Ventimiglia Flysch Fm. (For interpretation of the references to color in this figure legend, the reader is referred to the web version of this article.)

1 and about 10 m; Fig. 15C, D); 2) *Microcodium*-bearing nodular marly limestone with reworked globotruncanids (~4 m); 3) finely bedded, *Microcodium*-bearing, dark colored limestones with conglomerate lenses (10 to 20 m of thickness); 4) conglomerates characterized by clasts issued from both the Upper Cretaceous marlstones and the *Microcodium*-bearing conglomerates (~2 m of thickness); 5) dark colored marly limestones with vertebrate remains and pulmonate gastropods (~2 m of thickness); 6) pebble-rich

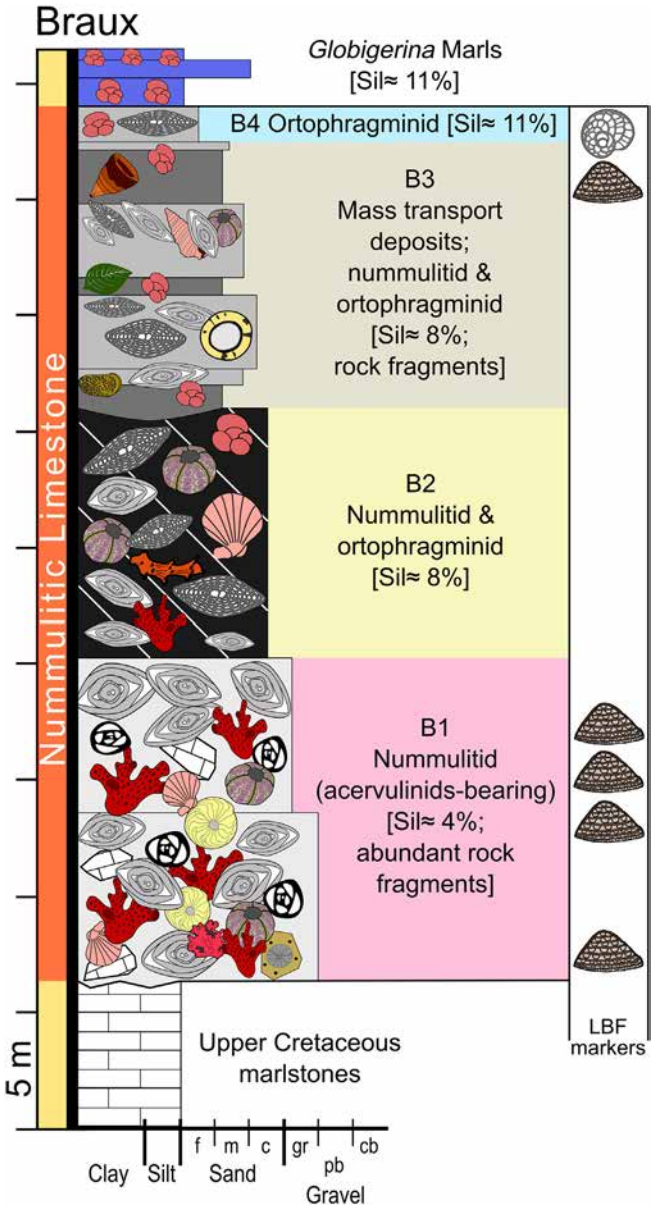

Fig. 10. Stratigraphic log of Braux section with information on skeletal assemblage and average grain-size. Symbols and abbreviations as in Fig. 3.

limestones, with schizohaline and shallow marine gastropods (~2 m of thickness).

The Nummulitic Limestone (12 m thick in the measured section) is relatively uniform, and consists of finely and irregularly bedded floatstones with a packstone matrix characterized by the nummulitid biofacies (Figs. 14, 15E). Macrofossils include lentil-sized *Nummulites*, including rare microspheric specimens up to 1 cm in diameter. Solitary corals, orthophragminids, gastropods, and bivalves are common (Fig. 15F, G). The skeletal assemblage is consistently dominated by LBF associated with echinoderms, mollusks, solitary corals and small benthic foraminifera (Fig. 16A, Table 1). *Nummulites* dominates the benthic foraminiferal assemblage and is associated with *Amphistegina* and *Operculina*; orthophragminids mainly occur in the upper part of the section (Fig. 16B, C). Small rotaliids and small miliolids are also present. Siliciclastic detritus including quartz, plagioclase, and abundant muscovite and chlorite increases up-section, whereas rock fragments (mainly reworked *Microcodium*) decrease (Fig. 14; Table 1).

The overlying *Globigerina* Marls consist of planktonic-foraminifera-rich impure mudstones containing mainly silt-sized quartz and plagioclase grains together with common muscovite and chlorite (Figs. 14, 16D; Table 1). The marls are followed by the Grès d'Annot turbidites.

5. Discussion

5.1. Biostratigraphy of the Nummulitic Limestone

The studied sections have been dated based on the distribution of the LBF fauna, focusing on the most readily identifiable biological events:

a) the extinction of *Assilina*, which took place in the Bartonian plankton zone P14 (40.0–38.0 Ma), following the 2011 calibration of Wade et al. (2011), Sartorio and Venturini (1988), Sztrákos and Du Fornel (2003), and Boudagher-Fadel (2018);
b) the common presence of *Chapmanina*, dated as within the shallow benthic zone SBZ18 of Serra-Kiel et al. (1998) (i.e., post-38 Ma);
c) the extinction of giant-sized nummulitids, considered to have occurred at the Bartonian–Priabonian boundary (~37.7 Ma; Nebelsick et al., 2005; Less and Özcan, 2012; Boudagher-Fadel, 2018; Özcan et al., 2019; Agnini et al., 2020);
d) the extinction of *Orbitolites*, also corresponding with the Bartonian–Priabonian boundary (Sartorio and Venturini, 1988; Serra-Kiel et al., 1998; Nebelsick et al., 2005; Boudagher-Fadel, 2018);
e) the first occurrence of *Heterostegina*, indicating the base of the Priabonian (Serra-Kiel et al., 1998; Boudagher-Fadel, 2018).

In the study area, the base of the Nummulitic Limestone was mainly considered as Bartonian (Sztrákos and Du Fornel, 2003; Varrone and Clari, 2003; Varrone and D'Atri, 2007). Thus, the presence of *Assilina*, *Orbitolites* and giant-size nummulitids indicates that the Mortola section deposited during the Bartonian and that the drowning of the carbonate factory here occurred before 38 Ma. The Loreto section also mostly deposited during the Bartonian, given the presence of not only giant-sized nummulitids, *Assilina* and *Orbitolites*, but also of large *Alveolina* specimens in the third interval. The large-sized representatives of this genus disappeared close to the end of the Bartonian (Serra-Kiel et al., 1998; Nebelsick et al., 2005; Less and Özcan, 2012). The presence of *Chapmanina*, however, indicates that the fifth interval of the Loreto section was deposited after 38 Ma. This is consistent with the local upper Bartonian/lower Priabonian planktonic foraminiferal assemblage of the *Globigerina* Marls (Varrone and D'Atri, 2007). The presence of both *Chapmanina* and giant-sized nummulitids dates the base of the Nummulitic Limestone in the Braux section as latest Bartonian (close to 38 Ma). The presence of the Priabonian taxa *Heterostegina* and *Discocyclina dispansa dispansa* (Less, 1987; Serra-Kiel et al., 1998) suggests a Priabonian age for the fourth interval. The Lauzanier section lacks diagnostic LBF taxa. The absence of either giant-sized nummulitids, *Assilina* and *Orbitolites* suggests deposition after 38 Ma, consistently with the Priabonian age proposed by Mulder et al. (2010) for the *Globigerina* Marls and the Grès d'Annot in this area.

5.2. Facies interpretation and paleoenvironmental reconstruction

Hallock and Glenn (1986), based on data on foraminiferal assemblages from modern and fossil tropical settings (Brasier, 1975a, 1975b; Hallock, 1980, 1983, 1984; Glenn et al., 1981; Hottinger, 1983a; Reiss and Hottinger, 1984), provided a general model of LBF distribution in carbonate depositional environments. Flat and thin large rotaliids (e.g. *Operculina*, *Heterostegina*, or orthophragminids like *Discocyclina*) dominate lower photic-zone assemblages, associated with common planktonic foraminifera. Thick and more robust nummulitids and robust amphisteginids (e.g. *Nummulites*, several species of *Amphistegina*) thrive in middle-shelf environments especially closer to the inner shelf. Very robust large rotaliids (e.g. several species of *Amphistegina*, *Miogypsina*)

Fig. 11. Braux section. A) Unconformable contact between Upper Cretaceous pelagic marlstones and Nummulitic Limestone (red arrow); B) B1, large nummulitids and echinoderms; C) B1, charcoal seam; D) overview of Braux section, red arrow = Upper Cretaceous marlstones, white arrows = nummulitic limestone intervals, green arrow = boundary between B2 and B3; E) B3, channelized surfaces (red arrow); F) B4, orthophragminid biofacies; G) resedimented layer in the lower *Globigerina* Marls. H) Upper part of Braux section, white arrow = B4, blue arrow = *Globigerina* Marls (blue arrow); yellow arrow = Grès d'Annot. (For interpretation of the references to color in this figure legend, the reader is referred to the web version of this article.)

dominate reef settings, whereas in even shallower water miliolids (e.g. alveolinids, soritids) are more abundant and can dominate in restricted environments. This model has been refined (e.g. Geel, 2000; Beavington-Penney and Racey, 2004; Boudaugher-Fadel, 2018), strengthened based on studies of modern assemblages (Van der Zwaan et al., 1990; Hohenegger, 1994, 2000, 2004; Hohenegger et al., 1999, 2000; Renema and Troelstra, 2001; Renema, 2006, 2018; Mateu-Vicens et al., 2009), and applied to diverse Cenozoic basins (e.g. Ćosović et al., 2004) including the Alpine foreland basin (Sinclair et al., 1998). Within this framework, we used our data on foraminiferal assemblages to constrain the environmental conditions in which each biofacies was deposited. The various biofacies of each section document a general deepening upward trend and a continuum of depositional environments with gradual transitions from one to another (e.g.

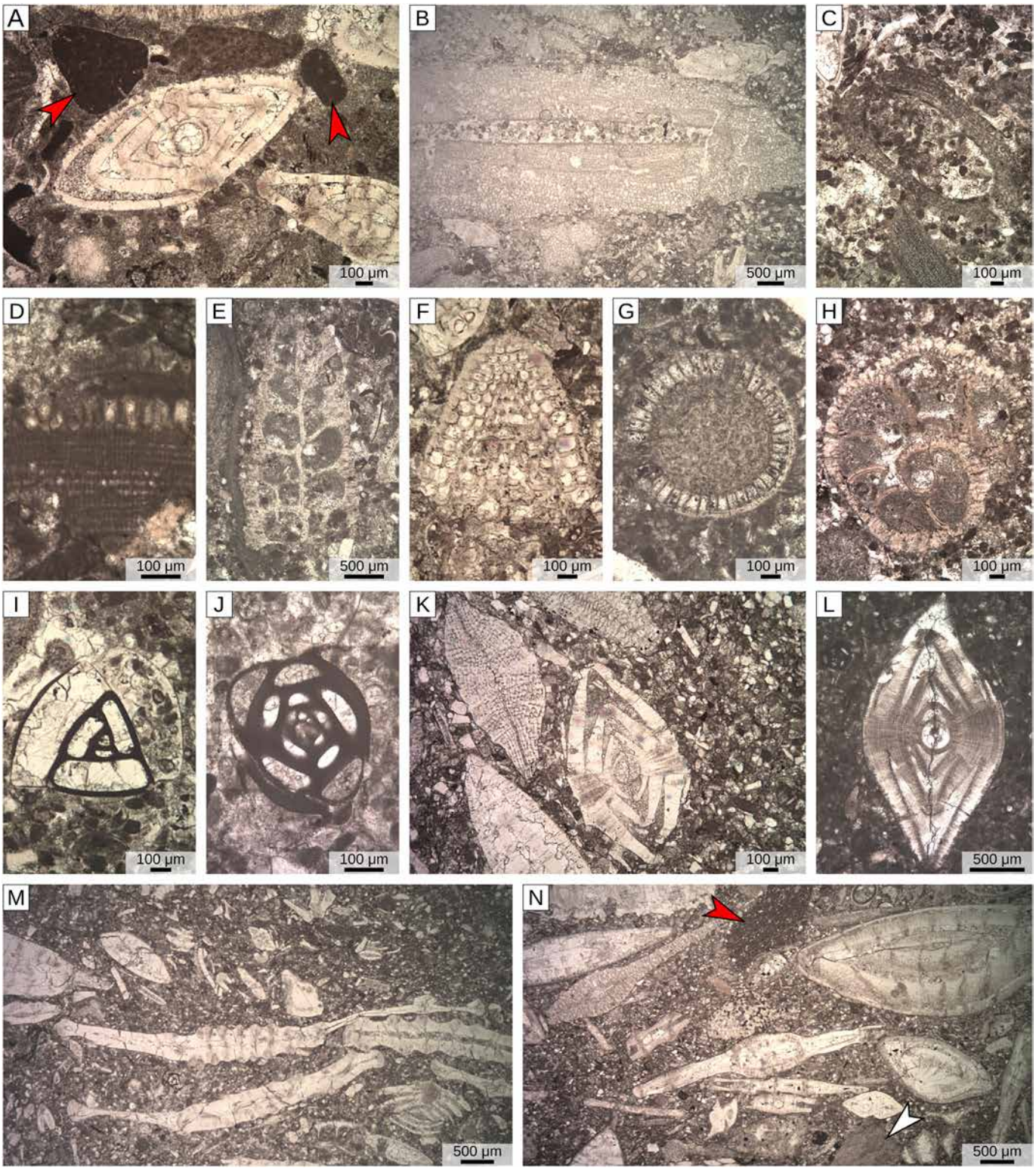

Fig. 12. Skeletal assemblage and microfossils in lower part of Braux section. A) B1, red arrows = clasts of Upper Cretaceous Marlstones; B, C) B1, large and small acervulinid nodules with hooked morphology; D) B1, *Sporolithon*; E) B1, bryozoan colony; F, G) B1, *Chapmanina*, axial and equatorial section respectively equatorial sections; H) B1, *Eorupertia*, equatorial section; I) B1, *Triloculina*; J) B1, *Quinqueloculina*; K) B2, nummulitid and orthophragminid biofacies; L) B2, *Nummulites*, axial section; M) B2, various specimens of *Operculina*; N) B3, imbricated fabric, red and white arrows point at clasts of Upper Cretaceous marls and of *Microcodium*, respectively. (For interpretation of the references to color in this figure legend, the reader is referred to the web version of this article.)

nummulitid and orthophragminid biofacies). The depositional system was thus characterized by a ramp profile. Ramps are actually common wherever carbonate factories mainly produce loose skeletal material rather than a rigid framework (i.e. a reef; Carannante et al., 1996; Schlager, 2005; Pomar, 2001; Pomar and Hallock, 2007; Pomar and Kendall, 2008; Williams et al., 2011). Lacking a marginal rim, Eocene ramps are characterized by unimpeded downslope transport and reworking processes (e.g. Beavington-Penney et al., 2005; Coletti et al.,

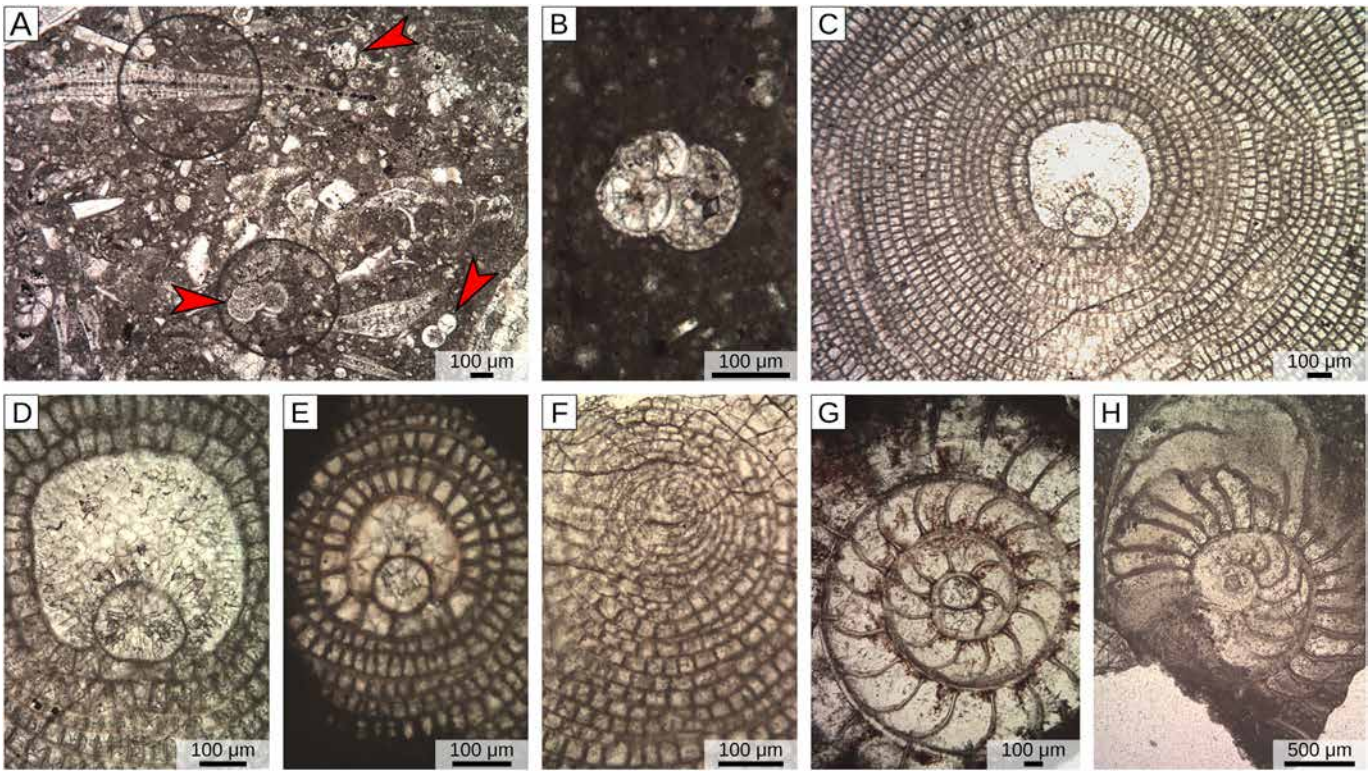

Fig. 13. Skeletal assemblage, microfossils, and oriented LBF specimens of B4. A) Overview of the orthophragminid biofacies, red arrows = planktonic foraminifera. B) Detail of a planktonic foraminifer. C) *Discocyclina dispansa dispansa*, megalospheric specimen, equatorial section (detail of embryo in D); E) other orthophragminid taxa; F) microspheric orthophragminid specimen exposing its early spiral stage. G) *Nummulites*, equatorial section. H) *Operculina* (possibly *O. gomezi* group), equatorial section. (For interpretation of the references to color in this figure legend, the reader is referred to the web version of this article.)

2016), as highlighted by the mass-transport deposits of the Loreto and Braux sections. The various biofacies can be ordered from shallowest to deepest.

The nummulitid biofacies (Mortola, Braux and Lauzanier sections) is characterized by grain-supported texture, abundance of thick and robust specimens of nummulitids, common presence of *Amphistegina* and miliolids, and scarcity of orthophragminids and planktonic foraminifera (Table 1), indicating a moderately high-energy, shallow water environment (indicatively between 20 and 40 m water depth). *Orbitolites* is remarkably similar to modern epiphytic soritids, and its presence is thus deemed indicative of a vegetated substrate (Brasier, 1975c; Beavington-Penney et al., 2006; Tomás et al., 2016; Tomassetti et al., 2016). The *Orbitolites*-bearing nummulitid biofacies of the Mortola section (Figs. 2B, 3, 5A) thus developed around a macrophyte meadow and because modern seagrasses occur in waters < 40 m and mostly <20 m deep (Duarte, 1991), water depth was probably around 20 m. The acervulinid-bearing nummulitid biofacies in the Braux section is characterized by hooked acervulinid crusts (Fig. 12B, C). Hooked and tubular morphologies in encrusting Eocene acervulinids have been linked to the presence of vegetated substrate (Tomás et al., 2016; Tomassetti et al., 2016), and seagrass encrusting acervulinids occurs in the recent (e.g. Langer, 1993; Wilson, 1998; Murray, 2006). Consequently, the acervulinid-bearing nummulitid biofacies of Braux are also interpreted as developed in close proximity to a vegetated substrate in a shallow environment (i.e., ~20 m water depth).

The acervulinid and coralline algal biofacies of the Loreto section is dominated by nodules of encrusting foraminifera (Fig. 6; Table 1). Modern acervulinids forming large macroids have been reported from the clear waters of the Gulf of Aqaba between 25 and 60 m of water depth (maximum abundance between 40 and 60 m below sea level; Hottinger, 1983b; Rasser and Piller, 1997), from the Florida shelf (35–65 m b.s.l.; Prager and Ginsburg, 1989), and from the Ryukyu Islands, where they occur between 60 and 105 m b.s.l. associated with *Operculina* and *Cycloclypeus* (Bassi et al., 2012, 2019). Loreto macroids are associated with large alveolinids (Fig. 9K), which only occur in this biofacies. The presence of small miliolids, *Orbitolites*, thick amphisteginids, the low abundance of orthophragminids, and the lack of planktonic foraminifera suggest deposition between 25 and 50 m of water depth.

The nummulitid and orthophragminid biofacies (Mortola and Braux sections) contains more orthophragminids, flat nummulitids and planktonic foraminifera, and less miliolids and amphisteginids than the nummulitid biofacies; grain size is finer, and textures mainly matrix-supported (Table 1). This biofacies overlies the nummulitid biofacies, documenting a deepening-upward trend and a transition to a moderately low-energy, middle shelf setting at depths indicatively between 40 and 60 m.

The coralline-algal branches and LBF biofacies in the Loreto section displays a foraminiferal assemblage similar to the nummulitids and to the nummulitid and orthophragminid biofacies (Table 1), indicating shallow to intermediate water depth. Similar skeletal assemblages, dominated by coralline algae but lacking either large rhodoliths or coralline algal bioconstructions, are common in the Eocene basins of eastern Italy and Austria and document inner to middle shelf environments (Nebelsick et al., 2005). A middle-shelf setting is also indicated by the diversified coralline algal assemblage including Sporolithales, Corallinales, and Hapalidiales (Adey, 1979, 1986; Minnery et al., 1985). Therefore, an environment with moderate hydrodynamic energy and water depth between 30 and 60 m is proposed.

The orthophragminid biofacies (Mortola and Braux sections) overlies the nummulitid and orthophragminid biofacies in the Mortola and Braux sections and is characterized by orthophragminids and other thin and flat LBF, common planktonic foraminifera, no miliolids, no amphisteginids, and abundant micrite (Table 1). This suggests a

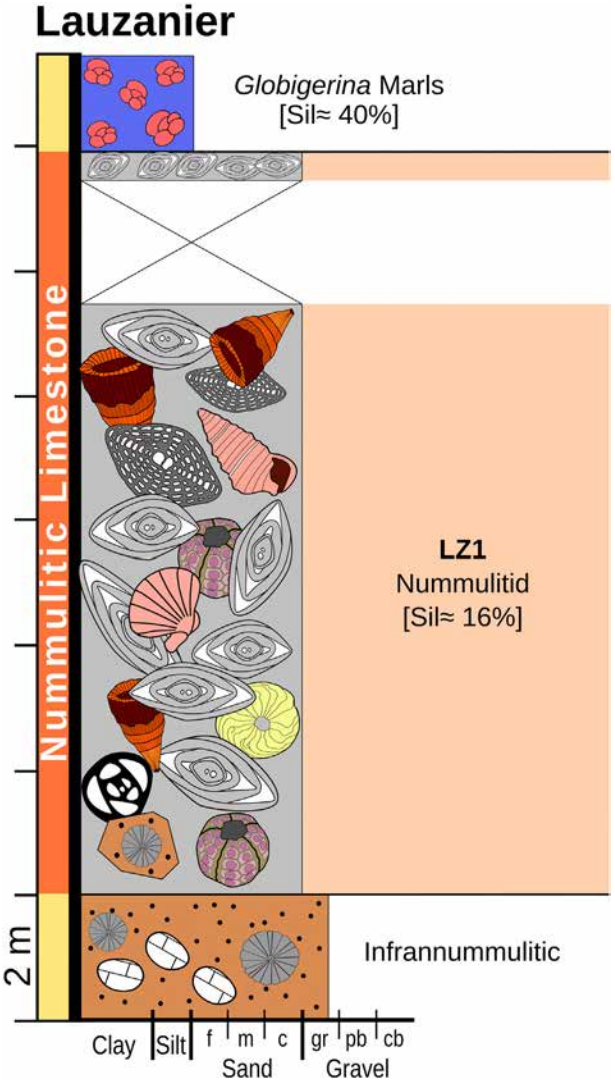

Fig. 14. Stratigraphic log of Lauzanier section with information on skeletal assemblage and average grain-size. Symbols and abbreviations as in Fig. 3.

below-wave base, outer shelf setting between ~60 m and the lowest limit of the photic zone (~100, 130 m maximum). Similarly to the orthophragminid facies, the orthophragminid and coralline algal biofacies of Loreto most likely developed in a similar outer shelf environment below wave base.

5.3. Controls on carbonate factories distribution

Sea-water temperature is considered a major control on the distribution of carbonate factories (e.g. Lees and Buller, 1972), however, the studied sections lie so close together that local temperature differences should not play a role in our case. The four sections were mostly deposited during the Bartonian (41.2–37.7 Ma), which was characterized by warm climate with a slow cooling trend culminated around the Eocene–Oligocene boundary (Zachos et al., 2001, 2008; Mosbrugger et al., 2005). The Bartonian also includes a warm peak, the Middle Eocene Climatic Optimum (c. 40.5–40.05 Ma; Zachos et al., 2008; Westerhold and Röhl, 2013). This event might have been recorded in the Mortola and Loreto sections. However, an overall large increase in thermophile taxa is not clearly documented in the skeletal assemblages.

Nutrient availability is another important control, together with autotrophs and symbiont-bearing organisms (e.g. LBF, hermatypic corals, calcareous algae) favored by oligotrophic conditions and heterotrophs (e.g. bryozoans, barnacles) favored by nutrient enrichment (Hallock and Schlager, 1986; Brasier, 1995a, 1995b). Such trend has been tested in both modern (Halfar et al., 2004; Reijmer et al., 2012; Reymond et al., 2016) and fossil carbonate systems (Coletti et al., 2017, 2019b). With the exception of the acervulinid and coralline algal biofacies, the four studied sections are dominated by autothrophs and symbiont-bearing organisms, with heterotroph carbonate producers (bryozoans in particular) occurring only as minor components. Little is known about the trophic preferences of Eocene acervulinids as their modern relatives seem to harbor no symbionts (Leutenegger, 1984). Within the study area, acervulinids are mainly related to shallow-water facies and are associated with light-loving taxa (e.g. *Alveolina*), suggesting a preference toward clear water rather than toward turbid (and possibly nutrient-rich) conditions. Overall, due to the abundance of terrigenous material (Table 1), it is likely that the foreland basin was enriched in nutrients in comparison to open oceanic conditions. However, by cross-comparing the various assemblage of the four sections there is no evidence indicating that nutrients exerted a primary control on the composition of the skeletal assemblages, possibly suggesting that if the basin was enriched in nutrients this enrichment was relatively uniform.

Major effects are ascribed to varying terrigenous supply. The Mortola and Lauzanier sections contain more terrigenous detritus and are overwhelmingly dominated by free-living benthic foraminifera, whereas coralline algae and encrusting foraminifera are more common at Loreto and Braux where siliciclastic supply was more limited (Table 1). A manifest difference results when sections or biofacies deposited at similar water depth (e.g. *Orbitolites*-bearing nummulitid biofacies of Mortola vs. acervulinid-bearing biofacies of Braux vs. acervulinid and coralline algal biofacies of Loreto) are compared (Table 1). Furthermore, by plotting all the samples containing remains of acervulinids, coralline algae and free-living benthic foraminifera, a negative correlation ($R^2 = 0.335$) can be observed between free-living benthic foraminifera (more abundant in impure limestones) and encrusting carbonate producers (foraminifera and coralline algae; more abundant in pure limestones; Fig. 17). The dominance of free-living benthic foraminifera in settings characterized by siliciclastic supply has been documented in Cenozoic basins of SE Asia and Spain (Lokier et al., 2009), showing that free-living benthic foraminifera tolerate terrigenous input better than coralline algae and hermatypic corals (which are the least tolerant carbonate producers). While Lokier et al. (2009) indicated coralline algae as the second most tolerant group, the distribution of coralline algae in our study suggests that Eocene calcareous red algae were relatively sensitive and fared better in clear waters. However, it should be noted that, while in the Neogene basins of SE Asia coralline algae frequently occur in samples containing >50% of clastic material, in the late Eocene of Spain the majority of coralline-bearing samples have <50% of clastics (Fig. 18) (Lokier et al., 2009). During the late Eocene, coralline algae, Hapalidiales and Corallinales in particular, became more abundant and more diversified (Aguirre et al., 2000; Nebelsick et al., 2005; Pomar et al., 2017), but our research focuses on relatively primitive middle Eocene assemblages largely consisting of Sporolithales. Therefore, it is conceivable that the studied middle Eocene algae were less flexible than their late Eocene and Neogene counterparts, and thus unable to flourish under very high rates of terrigenous sedimentation. Terrigenous supply exerted a significant influence also on secondary producers like solitary scleractinian corals, which are well adapted to high and persistent terrigenous input (Sanders and Baron-Szabo, 2005). This explains their common presence in the Mortola and Lauzanier sections that are rich in fine-grained terrigenous detritus (Table 1). The distribution of solitary corals, carefully investigated in the Mortola section by Carbone et al. (1980), has been shown to be dependent on the grain-size of terrigenous detritus: corals specialized in the removal of silt are more common in finer layers whereas species able to deal also with coarser particles prevail in coarser layers.

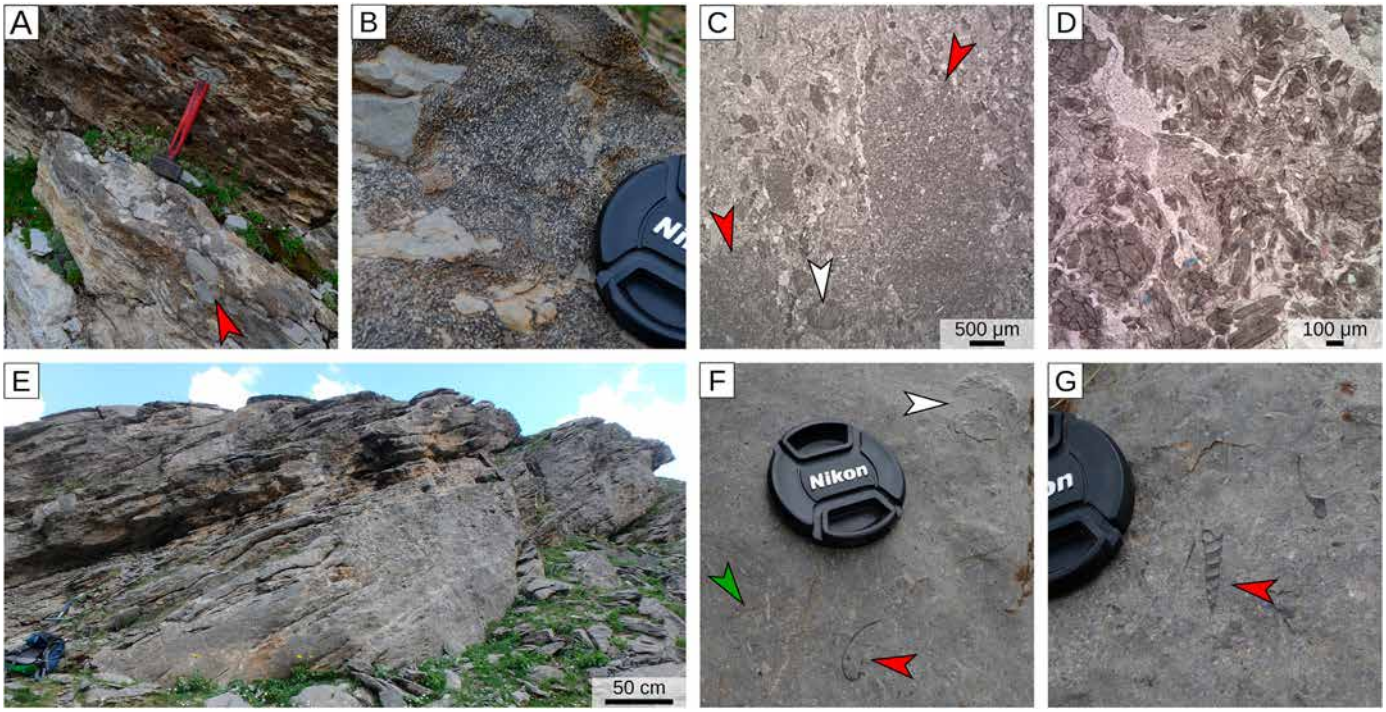

Fig. 15. Lauzanier section. A) Infranummulitic, conglomerate with clasts of Upper Cretaceous marlstones (red arrow); B) detail showing *Microcodium*; C) thin section of the Infranummulitic rocks, white and red arrows point at *Microcodium* and clasts of Upper Cretaceous marlstones, respectively; D) Infranummulitic, *Microcodium* in thin section; E) overview of the Nummulitic limestone section; F) Nummulitic Limestone, green arrow = orthophragminids, white arrow = solitary corals, red arrow = bivalve; G) Nummulitic Limestone gastropod (red arrow). (For interpretation of the references to color in this figure legend, the reader is referred to the web version of this article.)

Overall, two major carbonate factories, both dominated by benthic foraminifera, can be distinguished in the studied sections. Coastal areas closer to river outlets and thus characterized by greater terrigenous input and unstable substrates (e.g. Mortola, Braux and Lauzanier) were dominated by free-living LBF associated with other sediment-resistant taxa. Isolated banks (e.g., offshore shoals raised from the surrounding basin) characterized by limited terrigenous supply and more stable substrates (e.g., Loreto) hosted instead carbonate factories including more encrusting organisms (mostly foraminifera and coralline algae). The mineralogical analysis of the terrigenous fraction indicates the lack of minerals clearly related to high-grade Alpine metamorphic units, suggesting that the latter were probably not yet available for the erosion. This in turn might suggests a situation with limited relief around the basin during the development of the Nummulitic Limestone, with relatively localized input of material leading to the large differences in terrigenous content observed between the various outcrops.

6. Conclusions

Based on large benthic foraminiferal assemblages, the examined successions of the Nummulitic Limestone of Mortola, Loreto, Braux and Lauzanier deposited between the Bartonian and the Priabonian, with the former two depositing earlier.

Thanks to the analysis of the skeletal assemblage it was possible to recognize six main biofacies: i) the nummulitid biofacies and ii) the acervulinid and coralline algal biofacies both related to high-energy, moderately shallow water environment (20–40 m and 25–50 m respectively); iii) the nummulitid and orthophragminid biofacies and iv) the coralline-algal branches and LBF biofacies, related to slightly deeper settings (40–60 and 30–60 m respectively); v) the orthophragminid and the orthophragminid biofacies and vi) the orthophragminid and coralline algal biofacies related to even deeper water (60–130 m). These biofacies formed along a ramp profile testifying a progressively deepening of the depositional environment.

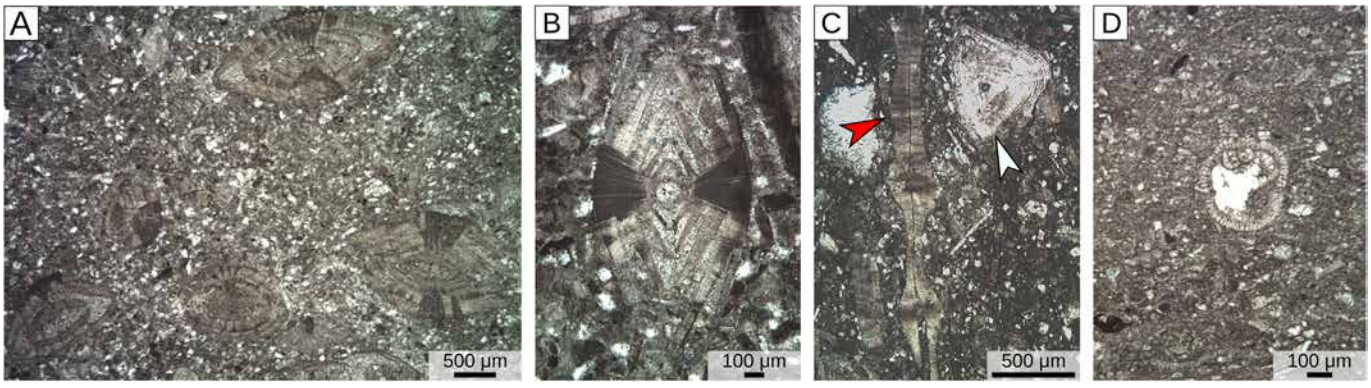

Fig. 16. Skeletal assemblage and microfossils in Lauzanier section. A) Overview of Nummulitid biofacies. B) *Nummulites*, axial section. C) *Operculina* (red arrow) and *Amphistegina* (white arrow). D) *Globigerina* Marls. (For interpretation of the references to color in this figure legend, the reader is referred to the web version of this article.)

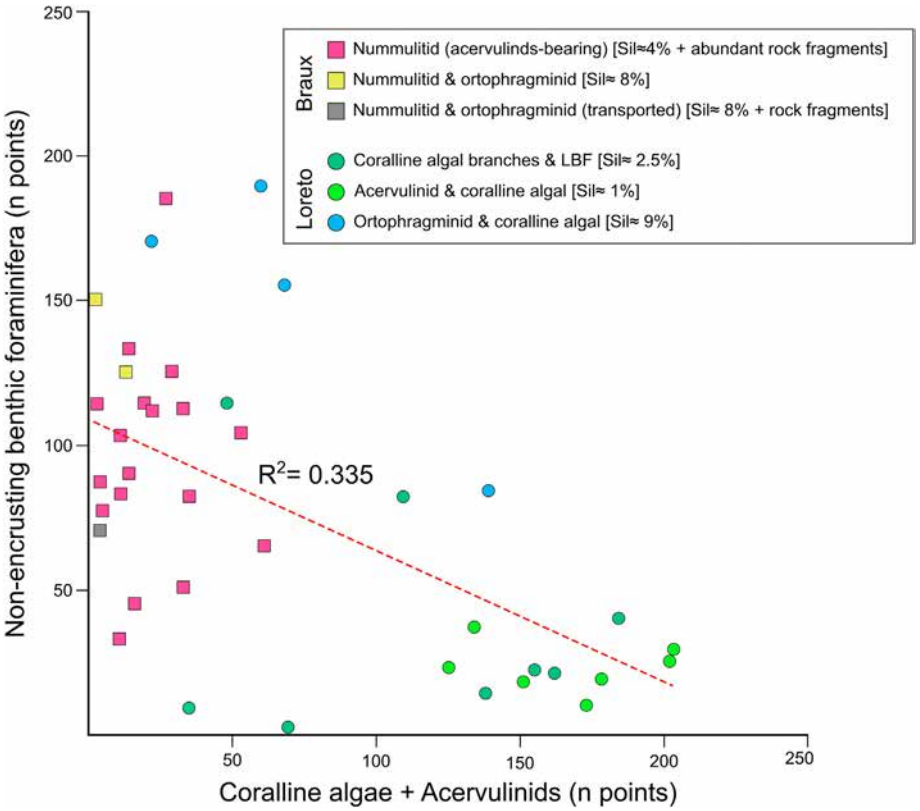

Fig. 17. Correlation between encrusting carbonate producers (coralline algae and encrusting acervulinids), free-living benthic foraminifera and terrigenous supply in the study area. Only samples displaying both encrusting carbonate producers (intended as coralline algae and encrusting acervulinids) and free-living benthic foraminifera were plotted.

These biofacies can be related to two major carbonate factories, the former dominated by free-living benthic foraminifera (Mortola, Braux and Lauzanier sections), and the latter dominated by coralline algae and encrusting foraminifera (Loreto section). Terrigenous supply exerted a primary control on these carbonate factories as encrusting organisms are significantly more common in pure limestones and free-living carbonate producers are much more common in areas characterized by a higher terrigenous supply like Mortola and Lauzanier. Free-living benthic foraminifera and solitary corals display more tolerance to clastic input than coralline algae and encrusting foraminifera. The distribution of coralline algae also suggests that Eocene algae might have been less tolerant to clastic input than their Neogene counterparts. Likewise, encrusting acervulinids seem to be mainly related to shallow water settings in the studied successions, and, therefore, relatively different from their modern counterparts that usually prefer deeper settings.

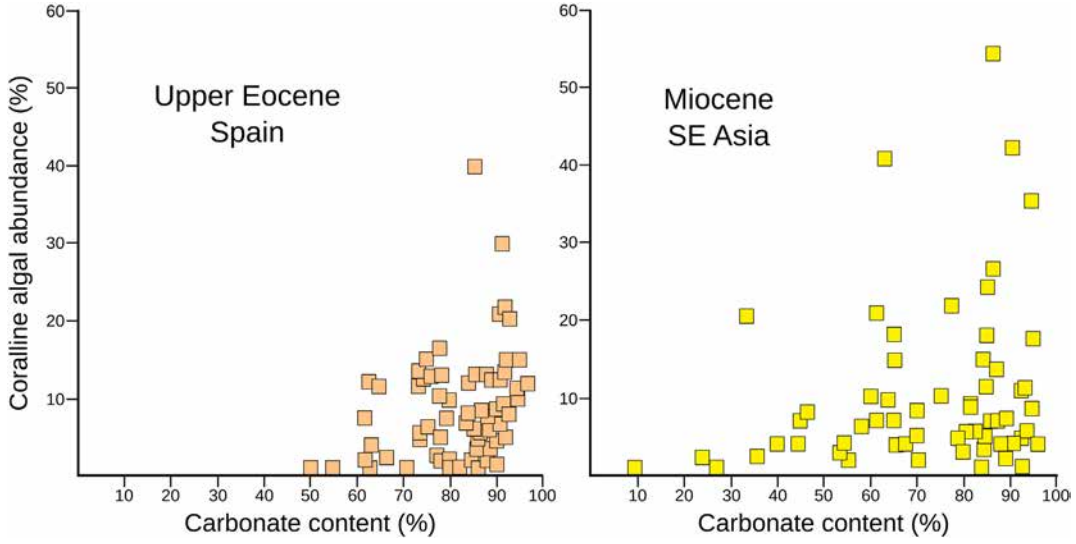

Fig. 18. Relationship between carbonate percentage and coralline algal abundance in samples from the upper Eocene of Spain and the Miocene of SE Asia investigated by Lokier et al. (2009) (data from the Supplementary material of Lokier et al., 2009).

This analysis highlights several differences between Paleogene and modern carbonate factories, but also indicates that, similarly to modern settings, terrigenous input represents a major controlling element of carbonate systems.

Supplementary data to this article can be found online at https://doi.org/10.1016/j.sedgeo.2021.106005.

Declaration of competing interest

The authors declare that they have no known competing financial interests or personal relationships that could have influenced the work reported in this paper.

Acknowledgements

The authors are grateful to Prof. Stani Giammarino for his guidance in this research and for providing the samples, collected during the field work of 1980 and previous campaigns, which were used for the analysis of the Mortola section. The authors wish to thank Prof. Cristina Carbone for the access to the PXRD laboratory of the University of Genoa, Roberto Badano is also acknowledged for his great help with PXRD analyses. The authors are grateful to Prof. György Less of Miskolc University and Prof. Giorgio Basilici of UNICAMP University for their constructive and helpful revisions. The first author is also indebted to Dr. Silvia Spezzaferri, Dr. Irene Cornacchia, Prof. Elisa Malinverno, Prof. Sergio Andò, Prof. Marco Malusà and Prof. Antonino Briguglio for the fruitful discussions on Eocene foraminifera and carbonates, and to Dr. Wendong Liang, Dr. Marta Barbarano, Mara Soldi, Maura Lenzi for their help during the fieldwork and labwork. The first author would also like to thank Milano-Bicocca University for funding its pots-doc grant. Finally, G.C. and E.G. would like to thank Curzio Malinverno for his invaluable help in thin sections preparation. This research represents a scientific contribution to Project MIUR - Dipartimenti di Eccellenza 2018–2022.

References

Adey, W.H., 1979. Crustose coralline algae as microenvironmental indicators in the Tertiary. In: Gray, J., Boucot, A.J. (Eds.), Historical Biogeography, Plate Tectonics and the changing environment. Proceedings of the thirty-seventh Annual Biology Colloquium, pp. 459-464.

Adey, W.H., 1986. Coralline algae as indicators of sea-level. In: Van de Plassche, O. (Ed.), Sea-level research: a manual for the collection and evaluation of data. Geo-Books, Norwich, pp. 229-280.

Agnini, C., Backman, J., Boscolo-Galazzo, F., Condon, D.J., Fornaciari, E., Galleotti, S., Giusberti, L., Grandesso, P., Lanci, L., Luciani, V., Monechi, S., Muttoni, G., Pälike, H., Pampaloni, M.L., Papazzoni, C.A., Pearson, P.N., Pignatti, J., Premoli-Silva, I., Raffi, I., Rio, D., Rook, L., Sahy, D., Spofforth, D.J.A., Stefani, C., Wade, B.S., 2020. Proposal for the Global Boundary Stratotype Section and Point (GSSP) for the Priabonian Stage (Eocene) at the Alano section (Italy). Episodes, doi: 10.18814/epiiugs/2020/020074.

Aguirre, J., Riding, R., Braga, J.C., 2000. Diversity of coralline red algae: origination and extinction patterns from the Early Cretaceous to the Pleistocene. Paleobiology, 26, 651-667.

Allen, P.A., Crampton, S.L., Sinclair, H.D., 1991. The inception and early evolution of the North Alpine Foreland Basin, Switzerland. Basin Research, 3, 143-163.

Allen, P.A., Burgess, P.M., Galewsky, J., Sinclair, H.D., 2001. Flexural-eustatic numerical model for drowning of the Eocene perialpine carbonate ramp and implications for Alpine geodynamics. GSA Bullettin, 113, 1052-1066.

Artoni, A., Meckel, L.D., 1998. History and deformation rates of a thrust sheet top basin. The Barrem basin, western Alps, SE France. In: Mascle, A., Puigdefabregas, C., Luterbacher, H.P., Fernandez, M. (eds.), Cenozoic Foreland Basins of Western Europe. Geological Society Special Publications, 134, 213-237.

Barale, L., Bertok, C., d'Atri, A., Martire, L., Piana, F., & Domini, G., 2016. Geology of the Entracque–Colle di Tenda area (Maritime Alps, NW Italy). Journal of Maps, 12, 359-370.

Bassi, D., Iryu, Y., Humblet, M., Matsuda, H., Machiyama, H., Sasaki, K., Matsuda S, Arai, K, Inoue, T., 2012. Recent macroids on the Kikai jima shelf, Central Ryukyu Islands, Japan. Sedimentology, 59, 2024-2041.

Bassi, D., Iryu, Y., Humblet, M., Matsuda, H., Machiyama, H., Sasaki, K., Matsuda, S, Arai, K, Inoue, T., 2019. Deep-Water Macroid Beds of the Ryukyu Islands, Japan: Encrusting Acervulinids as Ecosystem Engineers. Journal of Coastal Research, 35, 463-466.

Beavington-Penney, S.J., Racey, A., 2004. Ecology of extant nummulitids and other larger benthic foraminifera: applications in palaeoenvironmental analysis. Earth-Science Reviews, 67, 219-265.

Beavington-Penney, S. J., Paul Wright, V., Racey, A., 2005. Sediment production and dispersal on foraminifera-dominated early Tertiary ramps: the Eocene El Garia Formation, Tunisia. Sedimentology, 52, 537-569.

Beavington-Penney, S.J., Wright, V.P., Racey, A., 2006. The middle Eocene Seeb Formation of Oman: an investigation of acyclicity, stratigraphic completeness, and accumulation rates in shallow marine carbonate settings. Journal of Sedimentary Research, 76, 1137-1161.

Bernasconi, M.P., Corselli, C., Carobene, L., 1997. A bank of scleractinian coral *Cladocora caespitosa* in the Pleistocene of the Crati valley (Calabria, Southern Italy): growth vs environmental conditions. Bollettino della Società Paleontologica Italiana, 36, 53-61.

Bodelle, J., 1971. Les formations nummulitique de l'arc de Castellane. PhD Thesis, Université de Nice.

Boudaugher-Fadel, M.K., 2018. Evolution and geological significance of larger benthic foraminifera. UCL Press, 693 pp.

Brasier, M.D., 1975A. Ecology of Recent sediment-dwelling and phytal foraminifera from the lagoons of Barbuda, West Indies. The Journal of Foraminiferal Research, 5, 42-61.

Brasier, M.D., 1975B. The ecology and distribution of recent foraminifera from the reefs and shoals around Barbuda, West Indies. The Journal of Foraminiferal Research, 5, 193-210.

Brasier, M.D., 1975C. An outline history of seagrass communities. Palaeontology, 18, 681-702.

Brasier, M.D., 1995A. Fossil indicators of nutrient levels 1: eutrophication and climate change. In: Bosence, D.W.J., Allison, P.A. (Eds.), Marine Paleoenvironmental Analysis from Fossils. Geological Society Special Publication, 83, pp. 113–132.

Brasier, M.D., 1995B. Fossil indicators of nutrient levels 2: evolution and extinction in relation to oligotrophy. In: Bosence, D.W.J., Allison, P.A. (Eds.), Marine Paleoenvironmental Analysis from Fossils. Geological Society Special Publication, 83, pp. 133–150.

Campredon, R., 1977. Les formations paléogènes des Alpes Maritimes Franco-Italiennes. Mémoires de la Société Géologique de France, 9, 198 pp.

Carannante, G., Severi, C., Simone, L., 1996. Off-shelf carbonate transport along foramol (temperate-type) open shelf margins: an example from the Miocene of the central-southern Apennines (Italy). Mémoires de la Société géologique de France, 169, 277-288.

Carbone, F., Giammarino, S., Matteucci, R., Schiavinotto, F., Russo, A. 1980. Ricostruzione paleoambientale dell'affioramento nummulitico di Capo Mortola (Liguria Occidentale). Annali dell'Università di Ferrara, Scienze Geologiche e Paleontologiche, VI, 230-280.

Chung, F.H. 1974. Quantitative interpretation of X-ray diffraction patterns of mixtures. I. Matrix-flushing method for quantitative multicomponent analysis. Journal of Applied Crystallography, 7, 519–525.

Coletti, G., Vezzoli, G., Di Capua, A., Basso, D., 2016. Reconstruction of a lost carbonate factory based on its biogenic detritus (Ternate-Travedona Formation and Gonfolite Lombarda Group - northern Italy). Rivista Italiana di Paleontologia e Stratigrafia, 122, 1-22.

Coletti, G., El Kateb, A., Basso, D., Cavallo, A., Spezzaferri, S., 2017. Nutrient influence on fossil carbonate factories: Evidence from SEDEX extractions on Burdigalian limestones (Miocene, NW Italy and S France). Palaeogeography Palaeoclimatology Palaeoecology. 475, 80-92.

Coletti, G., Bosio, G., Collareta, A., Malinverno, E., Bracchi, V., Di Celma, C., Basso, D., Stainbank, S., Spezzaferri, S., Cannings, T., Bianucci, G. 2019A. Biostratigraphic, evolutionary, and paleoenvironmental significance of the southernmost lepidocyclinids of the Pacific coast of South America (East Pisco Basin, southern Peru). Journal of South American Earth Sciences, article #102372.

Coletti, G., Basso, D., Betzler, C., Robertson, A.H.F., Bosio, G., El Kateb, A., Foubert, A., Meilijson, A., Spezzaferri, S., 2019B. Environmental evolution and geological significance of the Miocene carbonates of the Eratosthenes Seamount (ODP Leg 160). Palaeogeography Palaeoclimatology Palaeoecology, 530, 217-235.

Ćosović, V., Drobne, K., Moro, A., 2004. Paleoenvironmental model for Eocene foraminiferal limestones of the Adriatic cabonate platform (Istrian Peninsula). Facies, 50, 61-75.

DeCelles, P.G., Giles, K.A., 1996. Foreland basin systems. Basin research, 8, 105-123.

Dickinson, W.R., 1974. Plate tectonics and sedimentation. In: Dickinson, W.R. (Ed.), Tectonics and Sedimentation. Society of Economic Paleontology and Mineralogy, Special Publication, 22, pp. 1–27.

Du Châtelet, É. A., Bout-Roumazeilles, V., Riboulleau, A., Trentesaux, A., 2009. Sediment (grain size and clay mineralogy) and organic matter quality control on living benthic foraminifera. Revue de micropaléontologie, 52, 75-84.

Duarte, C.M., 1991. Seagrass depth limits. Aquatic botany, 40, 363-377.

Evans, M.J., Elliott, T., 1999. Evolution of a thrust-sheet-top basin: The Tertiary Barreme basin. Alpes-de-haute-Provence, France. GSA Bullettin, 111, 1617-1643.

Doyle, L.J., Roberts, H.H., 1988. Carbonate–clastic Transitions. In: Developments in Sedimentology, 42, Elsevier, Amsterdam, 304 pp.

Dunham, R.J., 1962. Classification of carbonate rocks according to depositional texture. In: Ham, W.E. (Ed.), Classification of Carbonate Rocks. American Association of Petroleum Geologist, Memoire, 1, pp. 108–121.

Embry, A.F., Klovan, J.E., 1971. A Late Devonian reef tract on Northeastern Banks Island, NWT. Bulletin of Canadian Petroleum Geology, 19, 730–781.

Féraud, G., Ruffet, G., Stéphan, J.F., Lapierre, H., Delgado, E., Popoff, M., 1995. Nouvelles données géochronologiques sur le volcanisme paléogène des Alpes occidentales: existence d'un événement magmatique bref généralisé. Séance Spéciale de la Société géologique de France et de l‟ Association des Géologues du SE" Magmatismes dans le sud-est de la France", Nice, 25-26.

Flügel, E., 2010. Microfacies of Carbonate Rocks: Analysis Interpretation and Application. Springer, New York, 984 pp.

Ford, M., Lickorish, W.H., Kusznir, N.J. 1999. Tertiary foreland sedimentation in the Southern Subalpine Chains, SE France: a geodynamic appraisal. Basin Research, 11, 315-336.

Garzanti, E., 2019A. The Himalayan Foreland Basin from collision onset to the present: a sedimentary–petrology perspective. Geological Society, London, Special Publications, 483, 65-122.

Garzanti, E., 2019B. Petrographic classification of sand and sandstone. Earth-science Reviews, 192, 545-563.

Geel, T., 2000. Recognition of stratigraphic sequences in carbonate platform and slope deposits: empirical models based on microfacies analysis of Palaeogene deposits in southeastern Spain. Palaeogeography, Palaeoclimatology, Palaeoecology, 155, 211-238.

Giammarino, S., Fanucci, F., Orezzi, S., Rosti, D., Morelli, D., 2010. Foglio 258–271 San Remo. Note illustrative della carta geologica d'Italia alla scala 1:50.000. Servizio Geologico d'Italia, Roma, 136 pp.

Glenn, C., McManus, J.W., Talaue, L., Alino, P., Banzon, V., 1981. Distribution of live foraminifers on a portion of Apo Reef, Mindoro, Philippines. In Proceedings of the 4th International Coral Reef Symposium, Manila, 2, 775-781.

Gupta, S., 1997. Tectonic control on paleovalley incision at the distal margin of the early Tertiary Alpine Foreland Basin, Southeastern France. Journal of Sedimentary Research, 67, 1030-1043.

Gupta, S., Allen, P.A., 2000. Implications of foreland paleotopography for stratigraphic development in the Eocene distal Alpine foreland basin. GSA Bullettin, 112, 515-530.

Halfar, J., Godinez-Orta, L., Mutti, M., Valdez-Holguìn, J.E., Borges, J.M., 2004. Nutrient and temperature controls on modern carbonate production: an example from the Gulf of California. Mexico. Geology, 32, 213–216.

Hallock, P., 1980. Application of ecologic studies of living, algal symbiont-bearing foraminifera to paleoecologic interpretation. AAPG Bulletin, 64, 716-717.

Hallock, P., 1983. Larger foraminifera as depth indicators in carbonate depositional environments. AAPG Bulletin, 67, 477-478.

Hallock, P., 1984. Distribution of selected species of living algal symbiont-bearing foraminifera on two Pacific coral reefs. The Journal of Foraminiferal Research, 14, 250-261.

Hallock, P., Glenn, E.C., 1986. Larger foraminifera: a tool for paleoenvironmental analysis of Cenozoic carbonate depositional facies. Palaios, 1, 55-64.

Hallock, P., Schlager, W., 1986. Nutrient excess and the demise of coral reefs and carbonate platforms. Palaios, 1, 389–398.

Heikoop, J.M., Tsujita, C.J., Heikoop, C.E., Risk, M., Dickin, A., 1996. Effects of volcanic ashfall recorded in ancient marine benthic communities: comparison of a nearshore and an offshore environment. Lethaia, 29, 125–139.

Hohenegger, J., 1994. Distribution of living larger foraminifera NW of Sesoko Jima, Okinawa, Japan. Marine Ecology, 15, 291-334.

Hohenegger, J., Yordanova, E., Nakano, Y., Tatzreiter, F., 1999. Habitats of larger foraminifera on the upper reef slope of Sesoko Island, Okinawa, Japan. Marine Micropaleontology, 36, 109-168.

Hohenegger, J., 2000. Coenoclines of larger foraminifera. Micropaleontology, 46, 127-151.

Hohenegger, J., Yordanova, E., Hatta, A., 2000. Remarks on west Pacific Nummulitidae (foraminifera). The Journal of Foraminiferal Research, 30, 3-28.

Hohenegger, J., 2004. Depth coenoclines and environmental considerations of western Pacific larger foraminifera. The Journal of Foraminiferal Research, 34, 9-33.

Hottinger, L., 1983A. Processes determining the distribution of larger foraminifera in space and time. Utrecht Micropaleontological Bulletins, 30, 239-253.

Hottinger, L.K., 1983B. Neritic Macroid Genesis: an Ecological Approach. In: Peryt, T.M. (Ed.), Coated Grains. Springer-Verlag, Berlin, pp. 38–55.

Hu, X., Garzanti, E., Li, J., BouDagher-Fadel, M.K., Coletti, G., Ma, A., Liang, W., Xue, W., submitted. The “underfilled trinity” from the western Alpine foreland basin: reality or myth?.Tectonics.

James, N.P., Kendall, P., 1992. Introduction to carbonate and evaporite facies models. In: Walker, R.G., James, N.P. (Eds.), Facies Models: Response to Sea Level Change. Geological Association of Canada, Ontario, pp. 265–275.

Kabanov, P., Anadón, P., Krumbein, W.E., 2008. *Microcodium*: an extensive review and a proposed non-rhizogenic biologically induced origin for its formation. Sedimentary Geology, 205, 79-99.

Kempf, O., Pfiffner, O.A., 2004. Early Tertiary evolution of the North Alpine Foreland Basin of the Swiss Alps and adjoining areas. Basin Research, 16, 549-567.

Klappa, C.F., 1978. Biolithogenesis of Microcodium: elucidation. Sedimentology, 25, 489-522.

Košir, A., 2004. *Microcodium* revisited: root calcification products of terrestrial plants on carbonate-rich substrates. Journal of Sedimentary Research, 74, 845-857.

Langer, M.R., 1993. Epiphytic foraminifera. Marine Micropaleontology, 20, 235-265.

Lasker, H.R., 1980. Sediment rejection by reef corals: the roles of behavior and morphology in *Montastrea cavernosa* (Linnaeus). Journal of Experimental Marine Biology and Ecology, 47, 77-87.

Lees, A., Buller, A.T., 1972. Modern temperate-water and warm-water shelf carbonate sediments contrasted. Marine Geology, 13, M67-M73.

Less, G., 1987. Paleontology and stratigraphy of the European Orthophragminae. Geologica Hungarica, series Palaeontologica, 51, 1–373.

Less, G., Özcan, E., 2012. Bartonian-Priabonian larger benthic foraminiferal events in the western Tethys. Austrian Journal of Earth Sciences, 105, 129-140.

Leutenegger, S., 1984. Symbiosis in benthic foraminifera; specificity and host adaptations. The Journal of Foraminiferal Research, 14, 16-35.

Lickorish, W.H., Ford, M., 1998. Sequential restoration of the external Alpine Digne thrust system, SE France, constrained by kinematic data and synorogenic sediments. In: Mascle, A., Puigdefabregas, C., Luterbacher, H.P., Fernandez, M. (Eds.), Cenozoic Foreland Basins of Western Europe. Geological Society Special Publications, 134, pp. 189-211.

Lokier, S.W., Wilson, M.E.J., Burton, L.M., 2009. Marine biota response to clastic sediment influx: A quantitative approach. Palaeogeography Palaeoclimatology Palaeoecology, 281, 25-42.

Lokier, S.W., Al Junaibi, M., 2016. The petrographic description of carbonate facies: are we all speaking the same language?. Sedimentology, 63, 1843-1885.

Lüdmann, T., Kalvelage, C., Betzler, C., Fürstenau, J., Hübscher, C., 2013. The Maldives, a giant isolated carbonate platform dominated by bottom currents. Marine and Petroleum Geology, 43, 326-340.

Maino, M., Seno, S., 2016. The thrust zone of the Ligurian Penninic basal contact (Monte Frontè, Ligurian Alps, Italy). Journal of Maps, 12, 341-351.

Mateu-Vicens, G., Hallock, P., Brandano, M., 2009. Test shape variability of Amphistegina d'Orbigny 1826 as a paleobathymetric proxy: application to two Miocene examples. In: Demuchuck, T., Gary, A. (Eds.), Geologic problems solving with microfossils. SEPM special publication, 93, pp. 67-82.

Minnery, G.A., Rezak, R., Bright, T.J., 1985. Depth zonation and growth form of crustose coralline algae: Flower Garden Banks, Northwestern Gulf of Mexico. In: Toomey, D.F., Nitecki, M.H. (Eds.), Paleoalgology: Contemporary Research and Applications. Springer, New York, pp. 237-246.

Montenat, C., Leyrit, H., Gillot, P. Y., Janin, M. C., Barrier, P., 1999. Extension du volcanisme oligocène dans l'arc de Castellane (chaînes subalpines de Haute-Provence). Géologie de la France, 1, 43-48.

Mosbrugger, V., Utescher, T., Dilcher, D.L., 2005. Cenozoic continental climatic evolution of Central Europe. Proceedings of the National Academy of Sciences, 102, 14964-14969.

Mueller, P., Langone, A., Patacci, M., Di Giulio, A. 2018. Detrital signatures of impending collision: The deep-water record of the Upper Cretaceous Bordighera Sandstone and its basal complex (Ligurian Alps, Italy). Sedimentary Geology, 377, 147-161.

Mulder, T., Callec, Y., Parize, O., Joseph, P., Schneider, J.L., Robin, C., Dujoncquoy, E., Salles, T., Allard, J., Bonnel, C., Ducassou, E., Etienne, S., Ferger, B., Gaudin, M., Hanquiez, V., Linare, F., Marches, E., Toucanne, S., Zaragosi, S., 2010. High-resolution analysis of submarine lobes deposits: Seismic-scale outcrops of the Lauzanier area (SE Alps, France). Sedimentary Geology, 229, 160-191.

Murray, J.W., 2006. Ecology and applications of benthic foraminifera. Cambrige University Press, Cambridge, 426 pp.

Nebelsick, J.H., Rasser, M.W., Bassi, D., 2005. Facies dynamics in Eocene to Oligocene circumalpine carbonates. Facies, 51, 197-217.

Özcan, E., Less, G., Jovane, L., Catanzariti, R., Frontalini, F., Coccioni, R., Giorgioni, M., Rodelli, D., Rego, E.S., Kayğılı, S., Rostami, M.A., 2019. Integrated biostratigraphy of the middle to upper Eocene Kırkgeçit Formation (Baskil section, Elazığ, eastern Turkey): larger benthic foraminiferal perspective. Mediterranean Geoscience Reviews, 1, 55-90.

Perotti, E., Bertok, C., D'Atri, A., Martire, L., Piana, F., Catanzariti, R., 2012. A tectonically-induced Eocene sedimentary mélange in the Western Ligurian Alps, Italy. Tectonophysics, 568-569, 200-214.

Pomar, L., 2001. Ecological control of sedimentary accommodation: evolution from a carbonate ramp to rimmed shelf, Upper Miocene, Balearic Islands. Palaeogeography, Palaeoclimatology, Palaeoecology, 175, 249-272.

Pomar, L., Hallock, P., 2007. Changes in coral-reef structure through the Miocene in the Mediterranean province: Adaptive versus environmental influence. Geology, 35, 899-902.

Pomar, L., Kendall, C.G.StC., 2008. Architecture of carbonate platforms: a response to hydrodynamics and evolving ecology. In Controls on carbonate platform and reef development. SEPM Special Publication, 89, 187-216.

Pomar, L., Baceta, J.I., Hallock, P., Mateu-Vicens, G., Basso, D., 2017. Reef building and carbonate production modes in the west-central Tethys during the Cenozoic. Marine and Petroleum Geology, 83, 261-304.

Prager, E.J., Ginsburg, R.N., 1989. Carbonate nodule growth on Florida's outer shelf and its implications for fossil interpretations. Palaios, 4, 310-312.

Rasser, M.W., Piller, W.E., 1997. Depth distribution of calcareous encrusting associations in the northern Red Sea (Safaga, Egypt) and their geological implications. Proceedings of the 8th international Coral Reef Symposium, 743-748.

Ravenne, C., Vially, R., Riché, P., Trémolières, P., 1987. Sédimentation et tectonique dans le bassin marin Éocène supérieur – Oligocène des Alpes du Sud. Revue de L'Institut Français du Pétrole, 42, 529-553.

Reijmer, J.J.G., Bauch, T., Schäfer, P., 2012. Carbonate facies patterns in surface sediments of upwelling and non-upwelling shelf environments (Panama, East Pacific). Sedimentology, 59, 32-56.

Reiss, Z., Hottinger, L., 1984. The Gulf of Aqaba: ecological micropaleontology. Springer-Verlag, 354 pp.

Renema, W., Troelstra, S.R., 2001. Larger foraminifera distribution on a mesotrophic carbonate shelf in SW Sulawesi (Indonesia). Palaeogeography, Palaeoclimatology, Palaeoecology, 175, 125-146.

Renema, W., 2006. Habitat variables determining the occurrence of large benthic foraminifera in the Berau area (East Kalimantan, Indonesia). Coral Reefs, 25, 351.

Renema, W., 2018. Terrestrial influence as a key driver of spatial variability in large benthic foraminiferal assemblage composition in the Central Indo-Pacific. Earth-Science Reviews, 177, 514-544.

Reymond, C.E., Zihrul, K.S., Halfar, J., Riegl, B., Humphreys, A., Hildegard, W., 2016. Heterozoan carbonates from the equatorial rocky reefs of the Galapagos Archipelago. Sedimentology, 63, 940-958.

Roberts, H.H., 1987. Modern carbonate-siliciclastic transitions: humid and arid tropical examples. Sedimentary Geology, 50, 25-65.

Sanders, D., Baron-Szabo, R.C., 2005. Scleractinian assemblages under sediment input: their characteristics and relation to the nutrient input concept. Palaeogeography, Palaeoclimatology, Palaeoecology, 216, 139-181.

Sartorio, D., Venturini, S., 1988. Southern Tethys biofacies. Agip, 235 pp.

Serra-Kiel, J., Hottinger, L., Caus, E., Drobne, K., Ferrandez, C., Jauhri, A.K., Less, G., Pavlovec, R., Pignatti, J., Samso, J.M., Schaub, H., Sirel, E., Strougo, A., Tambareau, Y., Tosquella, J., Zakrevskaya, E., 1998. Larger foraminiferal biostratigraphy of the Tethyan. Bulletin de la Société géologique de France, 169, 281-299.

Schaffer, W., 1972. Ecology and paleoecology of marine environments. The University of Chicago Press, Chicago, 568 pp.

Schiller, C., 1993. Ecology of the symbiotic coral *Cladocora caespitosa* (L.) (Faviidae, Scleractinia) in the Bay of Piran (Adriatic Sea): I Distribution and biometry. Marine Ecology, 14, 205-219.

Schlager, W., 2005. Carbonate sedimentology and sequence stratigraphy (No. 8). SEPM Society for Sedimentary Geology, 206 pp.

Sinclair, H.D., 1997. Tectonostratigraphic model for underfilled peripheral foreland basins: An Alpine perspective. Geological Society of America Bulletin, 109, 324-346.

Sinclair, H.D., Sayer, Z.R., Tucker, M.E., 1998. Carbonate sedimentation during early foreland basin subsidence: the Eocene succession of the French Alps. In: Wrigth, V.P., Bruchette, T.P. (Eds.), Carbonate Ramps. Geological Society, London, Special Publications, 149, pp. 205-227.

Sinclair, H.D., Naylor, M., 2012. Foreland basin subsidence driven by topographic growth versus plate subduction. Bulletin, 124, 368-379.

Smith, A.M., 1995. Palaeoenvironmental interpretation using bryozoans: a review. Geological Society, London, Special Publications, 83, 231-243.

Sturani, C., 1965. Presence de Palaeotherium et de pulmones dans l'Eocene Continental du Lauzanier. Geologie Alpine, 41, 229-246.

Sztrákos, K., Du Fornel, E., 2003. Stratigraphie, paléoécologie et foraminifères du paléogène des Alpes Maritimes et des Alpes de Haute-Provence (Sud-Est de la France). Revue de Micropaléontologie, 46, 229-267.

Tomás, S., Frijia, G., Bömelburg, E., Zamagni, J., Perrin, C., Mutti, M., 2016. Evidence for seagrass meadows and their response to paleoenvironmental changes in the early Eocene (Jafnayn Formation, Wadi Bani Khalid, N Oman). Sedimentary Geology, 341, 189-202.

Tomassetti, L., Bosellini, F.R., Brandano, M., 2013. Growth and demise of a Burdigalian coral bioconstruction on a granite rocky substrate (Bonifacio Basin, south-eastern Corsica). Facies, 59, 703 - 716.

Tomassetti, L., Benedetti, A., & Brandano, M., 2016. Middle Eocene seagrass facies from Apennine carbonate platforms (Italy). Sedimentary Geology, 335, 136-149.

van den Hoeck, C., Mann, D.G., Jahns, H.M., 1995. Algae: an Introduction to Phycology. Cambridge University press, Cambridge, 623 pp.

Van der Zwaan, G.J., Jorissen, F.J., De Stigter, H.C., 1990. The depth dependency of planktonic/benthic foraminiferal ratios: constraints and applications. Marine Geology, 95, 1-16.

van Houten, F. B., 1973. Meaning of molasse. Geological Society of America Bulletin, 84, 1973-1976.

Varrone, D., Clari, P., 2003. Stratigraphic and paleoenvironmental evolution of the Microcodium Formation and the Numulitic Limestone in the French-Italian Maritime Alps. Geobios, 36, 775-786.

Varrone, D., D'Atri, A., 2007. Acervulinid macroid and rhodolith facies in the Eocene Nummulitic Limestone of the Dauphinois Domain (Maritime Alps, Liguria, Italy). Swiss Journal of Geosciences, 100, 503-515.

Varrone, D., Decrouez, D., 2007. Eocene larger foraminiferal biostratigraphy in the southernmost Dauphinois domain (Maritime Alps, France-Italy border). Rivista Italiana di Paleontologia e Stratigrafia, 113, 257-267.

Wade, B.S., Pearson, P.N., Berggren, W.A., Pälike, H., 2011. Review and revision of Cenozoic tropical planktonic foraminiferal biostratigraphy and calibration to the geomagnetic polarity and astronomical time scale. Earth-Science Reviews, 104, 111-142.

Westerhold, T., Röhl, U., 2013. Orbital pacing of Eocene climate during the Middle Eocene Climate Optimum and the chron C19r event: Missing link found in the tropical western Atlantic. Geochemistry Geophysics Geosystems, 14, 4811-4825.

Williams, H.D., Burgess, P.M., Wright, V.P., Della Porta, G., Granjeon, D., 2011. Investigating carbonate platform types: multiple controls and a continuum of geometries. Journal of Sedimentary Research, 81, 18-37.

Wilson, B., 1998. Epiphytal Foraminiferal Assemblages on the Leaves of the Seagrasses *Thalassia testudinum* and *Syringodium filiforme*. Caribbean Journal of Science, 34, 131-131.

Wilson, E.J.W, Lokier, S., 2002. Siliciclastic and volcaniclastic influences on equatorial carbonates: insights from the Neogene of Indonesia. Sedimentology, 49, 583-601.

Zachos, J., Pagani, M., Sloan, L., Thomas, E., Billups, K., 2001. Trends, rhythms, and aberrations in global climate 65 Ma to present. Science, 292, 686-693.

Zachos, J.C., Dickens, G.R., Zeebe, R.E., 2008. An early Cenozoic perspective on greenhouse warming and carbon-cycle dynamics. Nature, 451, 279-283.